

# Modeling of Radar Signatures of Wake Vortices in Rainy weather

**Directeur de thèse:**

VINCENT François (ISAE, France),  
JEANNIN Nicolas (ONERA, France)

**LIU Zhongxun**

**27<sup>th</sup> May, 2013**

- 1. Introduction**
- 2. Raindrop's motion and distribution**
- 3. Radar signatures simulation**
- 4. Radar signatures interpretation**
- 5. Conclusions and perspectives**



# 1. Introduction

- **1.1 Wake vortex hazards**
- **1.2 Airport capacity**
- **1.3 Candidate sensors for monitoring wake vortex**

### What is wake vortex

- A disturbance in the air that occurs when a wing is generating lift
  - the high-pressure air moves around the wingtip to the low pressure
- Two counter-rotating vortices
- Wake vortex strength: initial circulation

$$\Gamma_0 = \frac{Mg}{\rho U b_0}, \quad b_0 = \frac{\pi}{4} b$$

$M$ : aircraft weight  
 $U$ : flying speed  
 $b$ : aircraft's wingspan

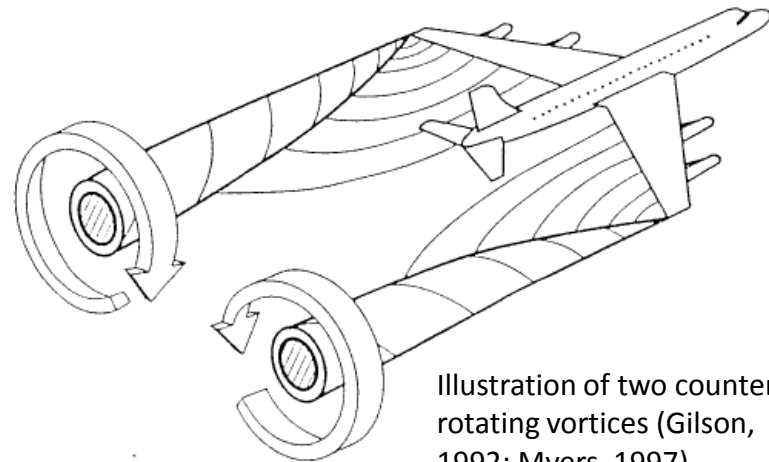
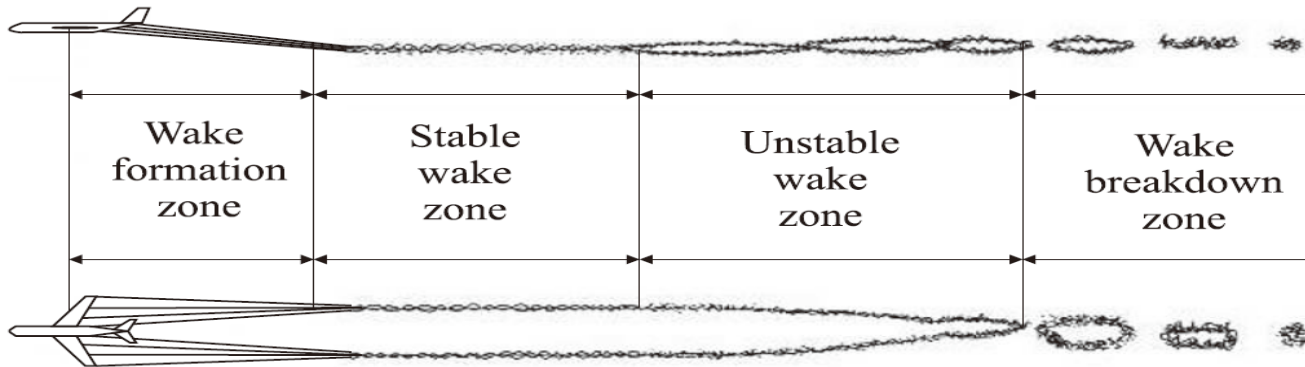


Illustration of two counter-rotating vortices (Gilson, 1992; Myers, 1997)

- Especially hazardous during take-off and landing

### Wake vortex evolution (Four Phases)



Ginevsky and Zhelannikov 2009

### Wake vortex can be made visible



Wake vortices of Learjet 60 in cloud (Photo by P. Bowen)



Wake vortices at high altitude as contrail

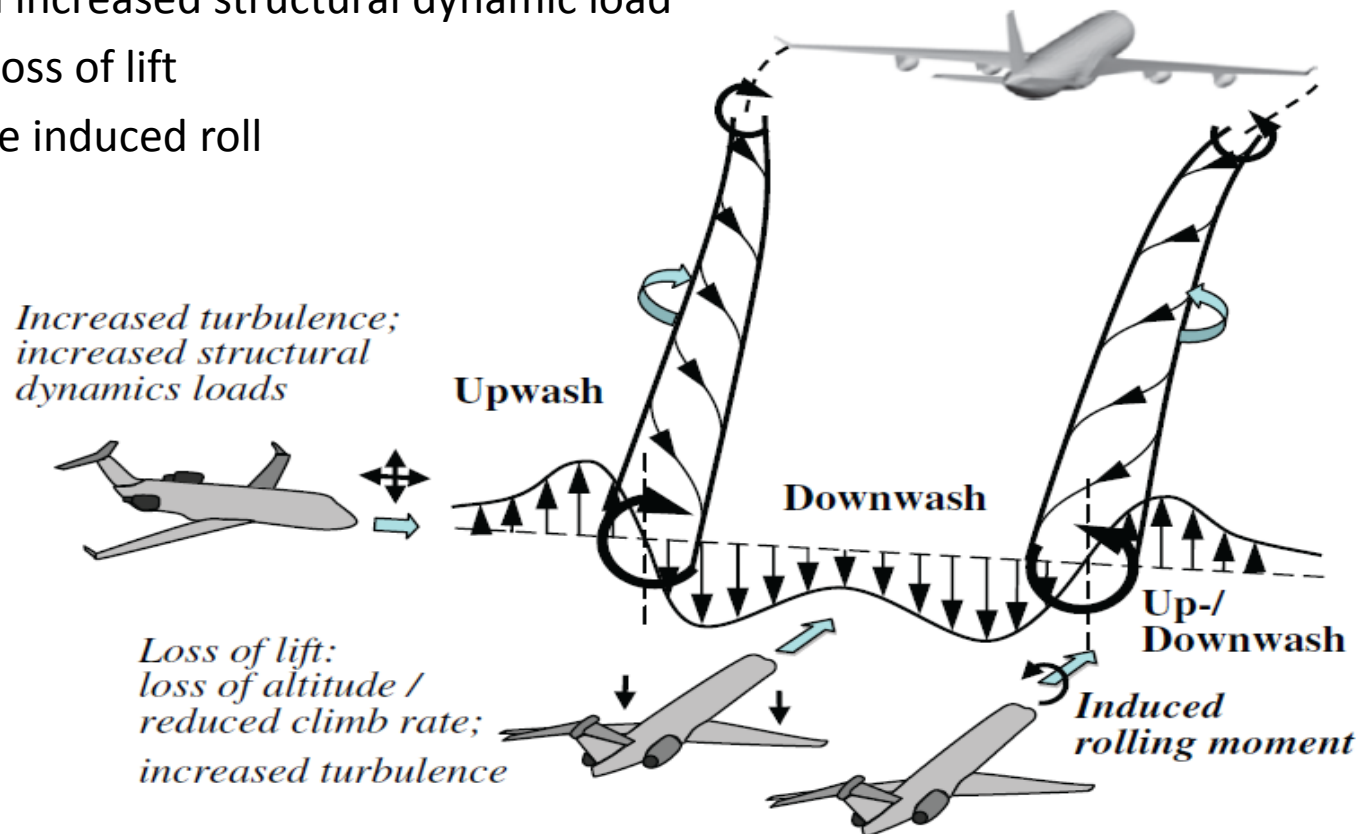


Wake vortices made visible in a NASA test by using colored smoke rising from the ground

- Large extension:
  - up to 30 kilometers behind the aircraft
- Long lifetime:
  - several minutes
- Large strength:
  - potential hazards

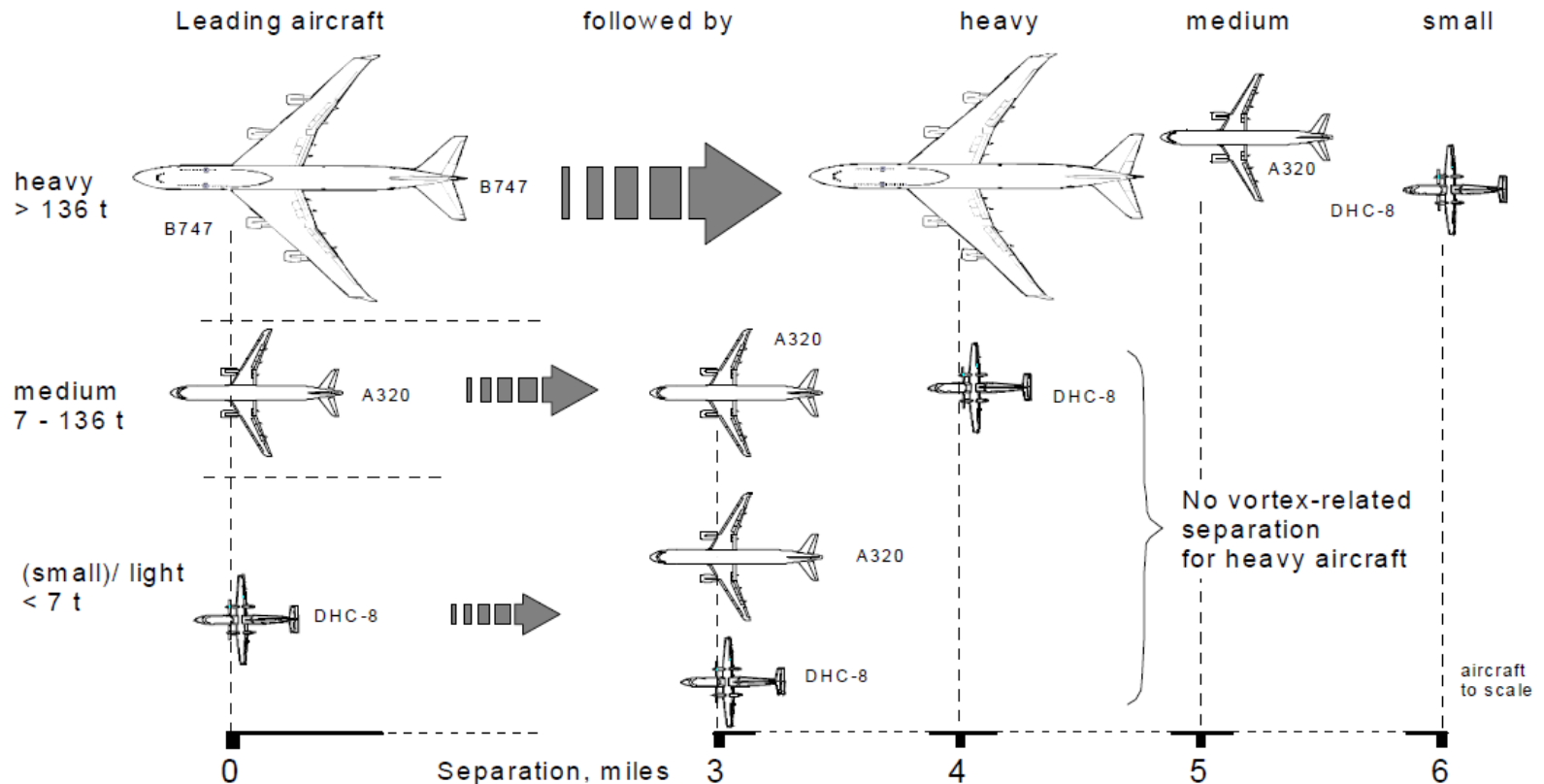
### Wake vortex encounters (Breitsamter, 2010)

- depending upon how the aircraft penetrates the wake vortex
- three main hazards caused by vortex encounters
  - an increased structural dynamic load
  - a loss of lift
  - the induced roll



### Current ICAO wake separation standards

- classification based on aircraft weight (implemented over 40 years ago)
- too conservative but not always safe (when wake vortex under cross wind or ground effect)



### EU project: **SESAR** (2004-2020)

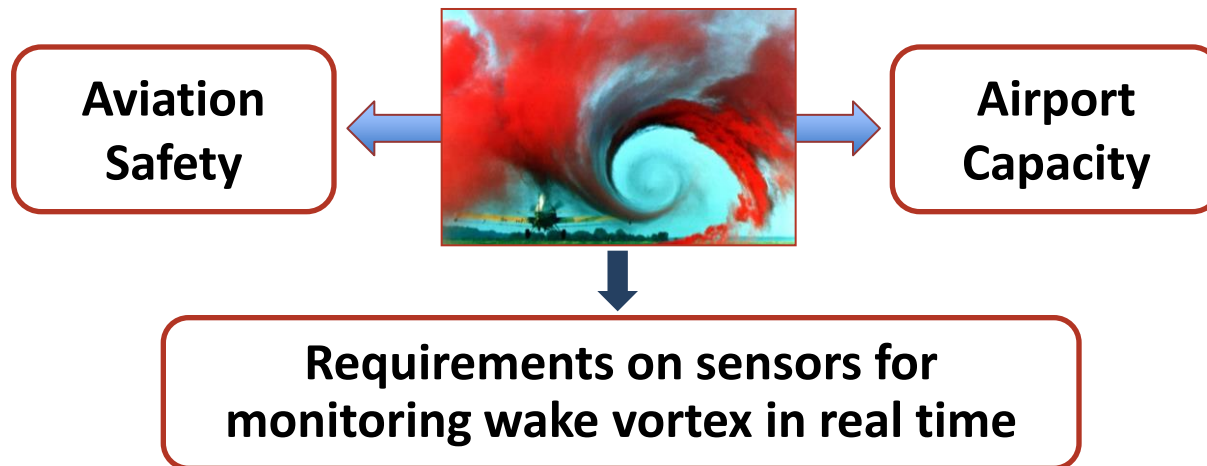
	by 2020	Long term
<b>CAPACITY</b>	+73%	×3
<b>SAFETY</b>	×3	×10



Single European Sky ATM Research

SESAR Project 12.2.2 :

*Runway Wake Vortex Detection, Prediction and decision support tools*





### LIDAR

### SODAR

### RADAR



Lockheed Martin



*OptiNav*



ASC



THALES



USDOT



NUDT

LIDAR---- the atmospheric aerosols in clear air (Mie scattering)

SODAR-- the temperature (or density) fluctuations

RADAR--- the refractive index fluctuations

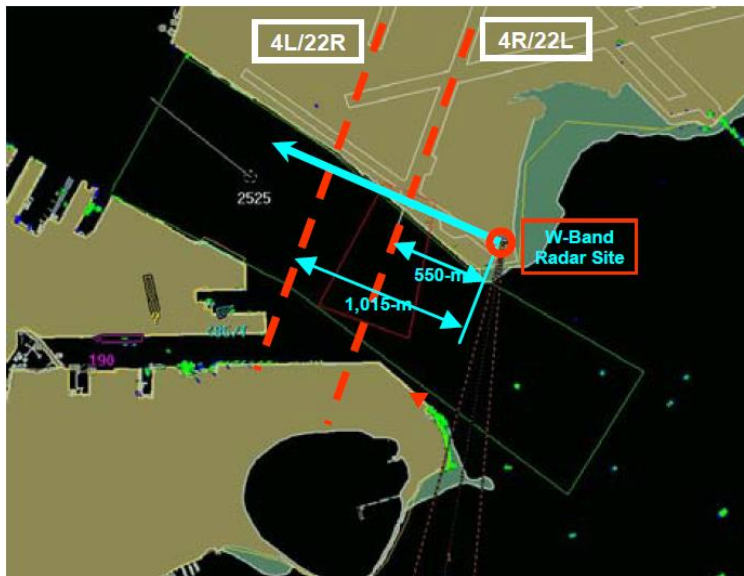
--- rain/fog droplets (Rayleigh or Mie scattering)

### Radar monitoring of wake vortex

- In clear air, radar reflectivity from wake vortex is extremely low
  - Experiment results:
    - Nespor et al. 1994 : C band
    - Shephard. 1990 : S and X band
  
- In rainy weather, raindrops are strong scatterers
  - Experiment results:
    - F. Barbaresco, 2012: X band Radar
    - T. A. Seliga, 2009: W band Radar

### W band radar trials in rain:

T. A. Seliga and J. B. Mead. Meter-scale observations of aircraft wake vortices in precipitation using a high resolution solid-state W-band radar. In The 34<sup>th</sup> conference on Radar Meteorology, 2009.

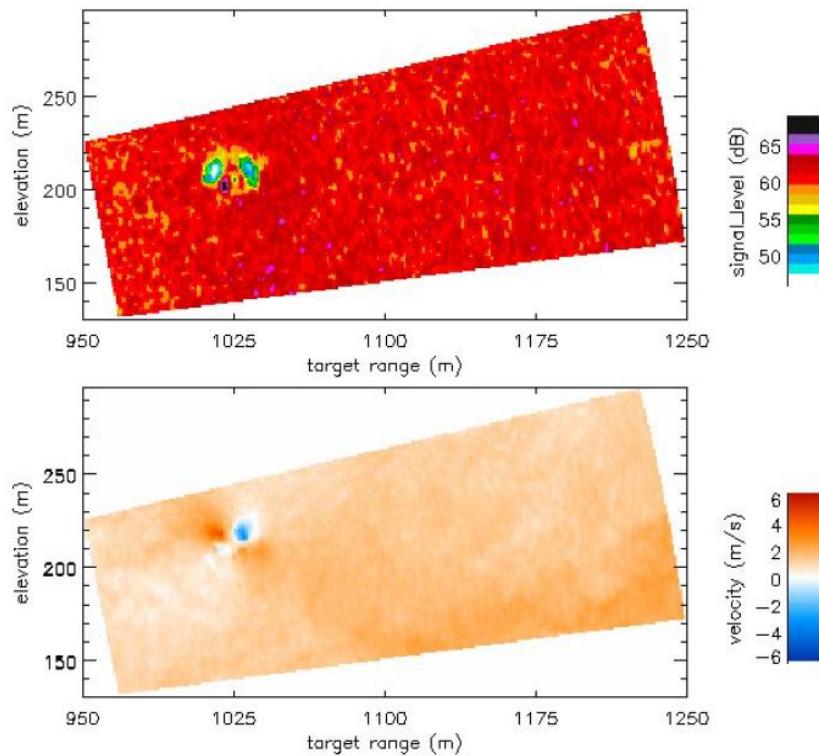


Location of the W-Band Radar at Boston's Logan Int. Airport

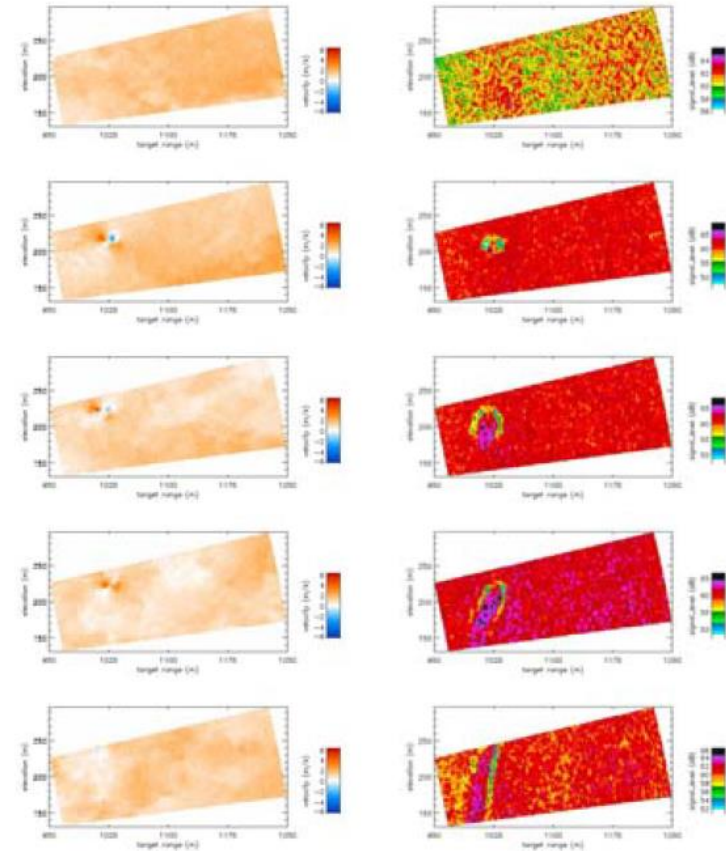
Parameter	Value
Frequency of Operation	94.0-94.25 GHz
Peak Transmit Power	100 mW
Waveform Type	Linear FM chirp
Range Resolution	1.0 m
Pulse Repetition Frequency	20 kHz
Pulse Duration (min- max)	1-10 $\mu$ s
Antenna Diameter & Type	48" Cassegrain
Antenna Beamwidth	0.18°
Antenna Gain	58 dB
Front-end Noise Figure	12 dB

W-Band Radar parameters

### W band radar trials in rain (2009):



Peak spectral power level of the signal within each range bin, and peak Doppler velocity

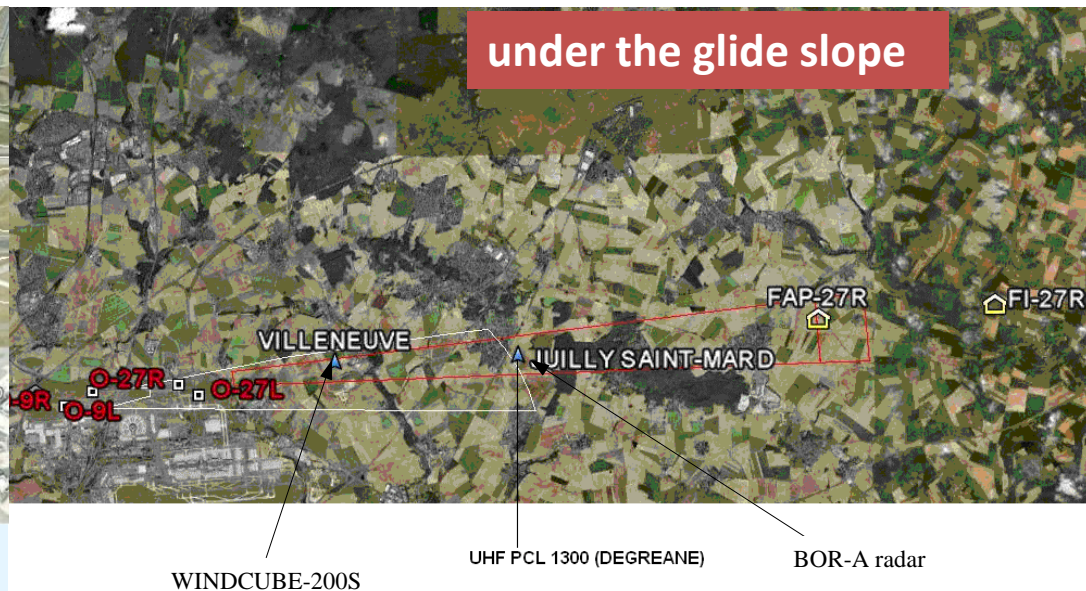


Time history of the wake vortices detected by the W-Band Radar on March 26, 2009

### X band radar trials in rain (2012):

F. Barbaresco. Radar/Lidar Sensors for Wind & Wake-Vortex Monitoring on Airport: First results of SESAR P12.2.2 XP0 trials campaign at Paris CDG Airport. In WakeNet3-Europe 4th Major Workshop "Wake Turbulence in Current Operations and Beyond", 2012.

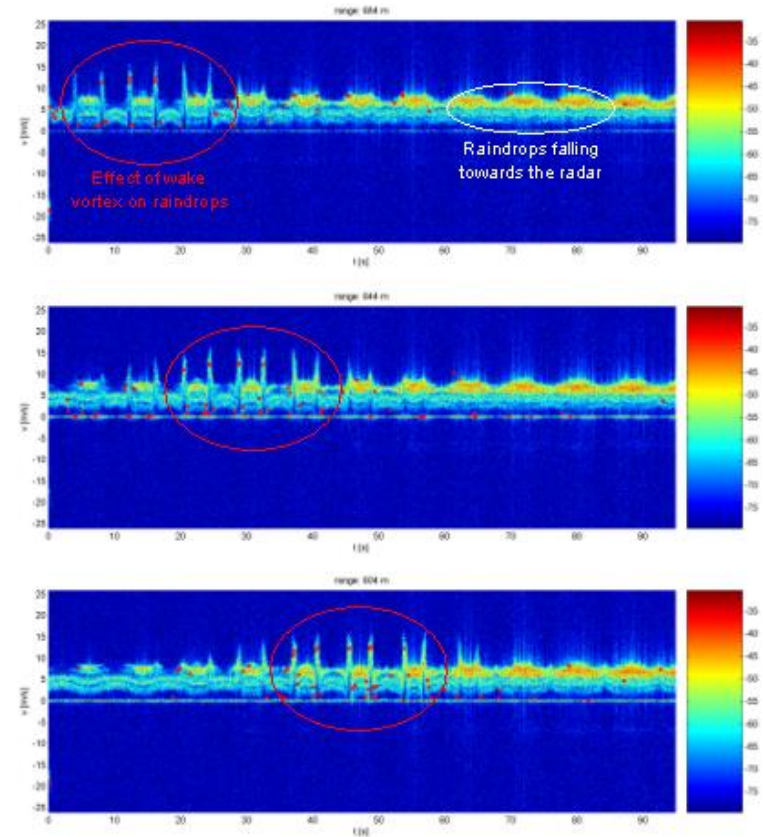
### Wake-Vortex Sensors Deployment



### X band radar trials in rain (2012):

#### X band radar parameters

Parameters	Values
Radar frequency	10 GHz
Transmitted peak power	20 W
Noise figure	2 dB
System Loss	3 dB
Antenna gain	30 dB
Beam width	$2.8^\circ \times 4^\circ$
Distance to the wake vortex	500 m
Pules Repetition Frequency	3348 Hz
Number of pulses	256

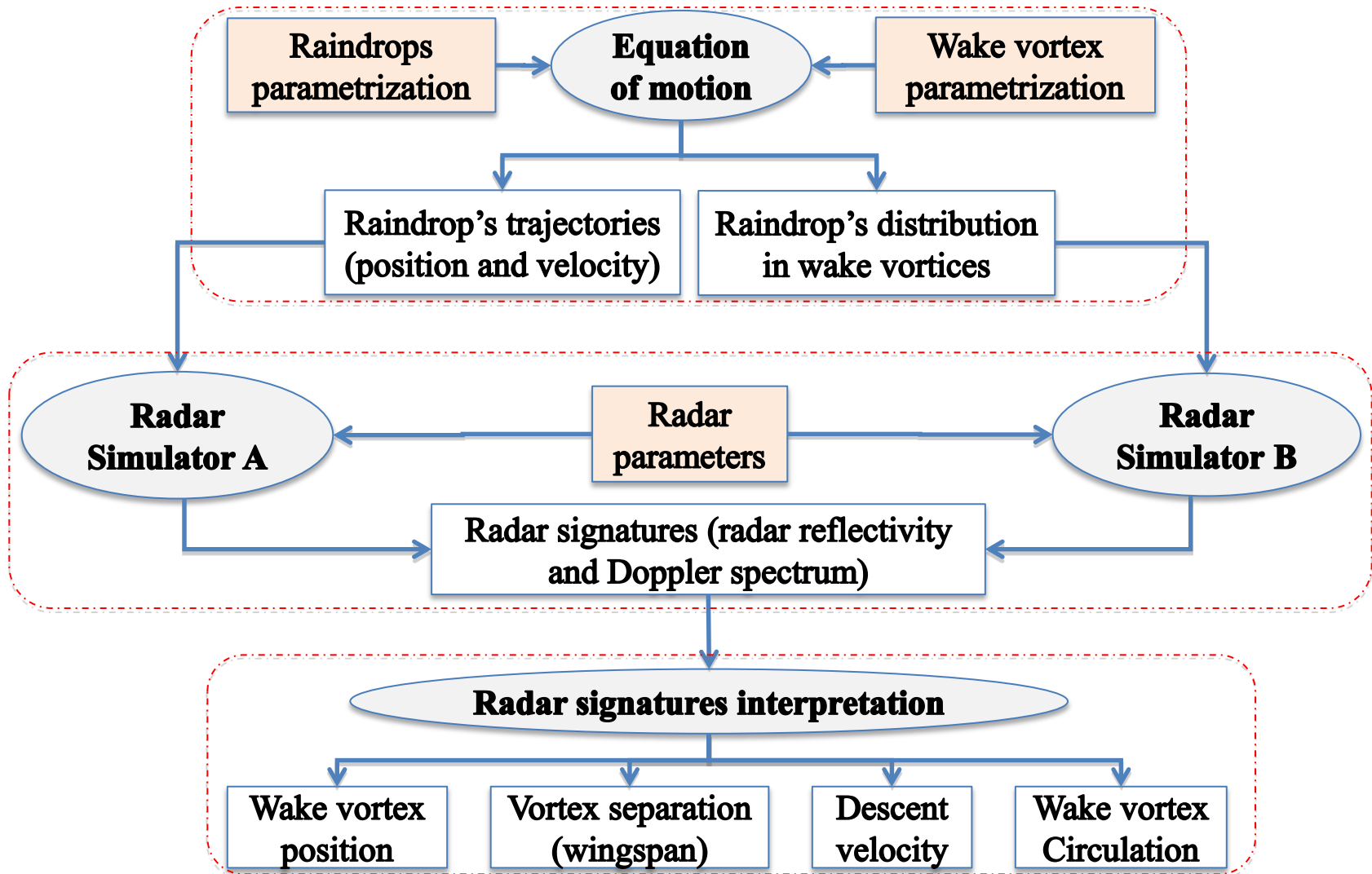


Time Doppler spectrum of raindrops in three successive radar cells

Radar is a potential sensor for monitoring wake vortex in rain, very few research has been reported until now to model and evaluate the radar signatures of wake vortex in rainy weather.

Thus, some critical problems arising from this requirement need to be studied:

- **Raindrops' motion and distribution in wake vortices;**
- **Radar signatures of raindrops in wake vortex;**
- **Interpretation of wake vortex radar signatures.**



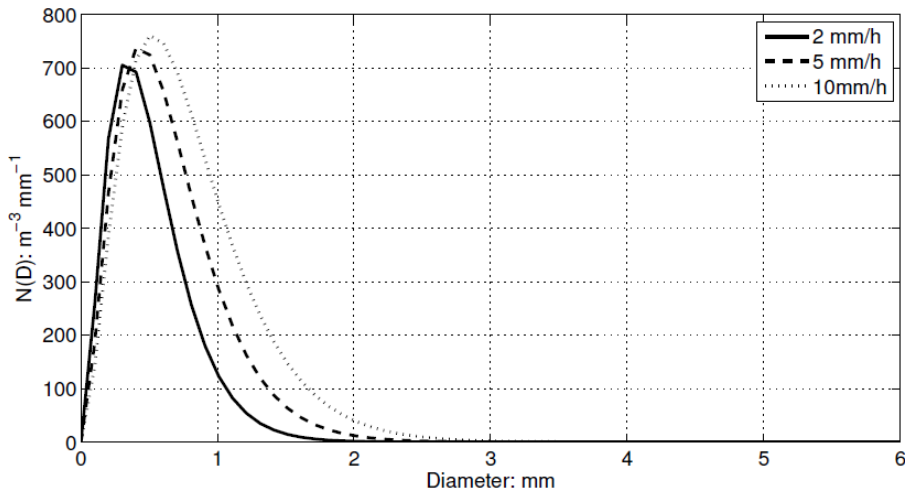




## 2. Raindrops' motion and distribution

- 2.1 Parametrization of raindrops
- 2.2 Wake vortex velocity field
- 2.3 The equation of motion
- 2.4 Raindrop's trajectory in wake vortices
- 2.5 Raindrop's distribution in wake vortices

### Raindrop size distribution



$$N(D) = N_0 D^2 e^{-\Lambda D}, \quad (m^{-3}mm^{-1})$$

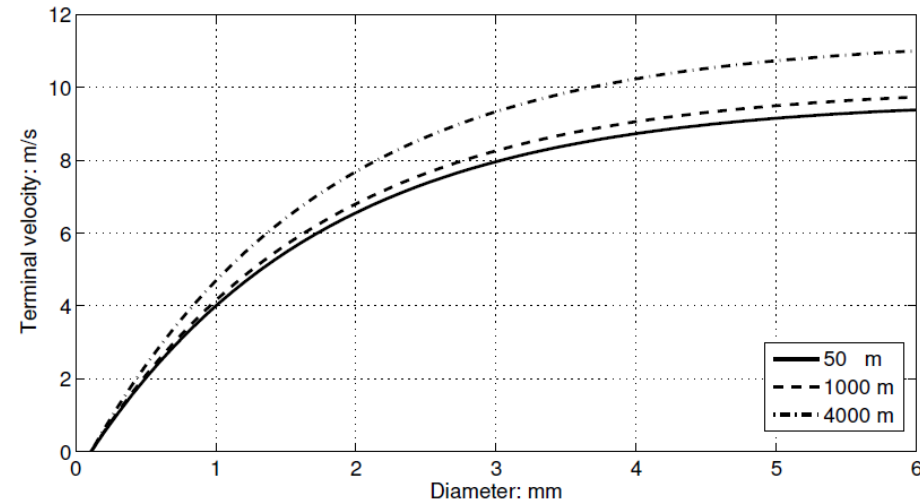
$$N_0 = 64500 R^{-0.5} \quad (\text{in } m^{-3}mm^{-3}), \quad (\text{Atlas and Ulbrich 1974; Owolawi 2010})$$

$$\Lambda = 7.09 R^{-0.27} \quad (\text{in } mm^{-1}),$$

### Assumptions for Raindrops:

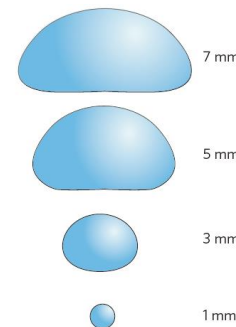
- ✓ spherical and not deformable
- ✓ no collision or coalescence
- ✓ no significant evaporation or condensation

### Raindrop's terminal falling velocity



$$V_T(D) = [\alpha_1 - \alpha_2 \exp(-\alpha_3 D)] \left( \frac{\rho_0}{\rho} \right)^{0.4}$$

D. Atlas, R. C. Srivastava, and R. S. Sekhon 1973;  
V. N. Bringi and V. Chandrasekar 2004



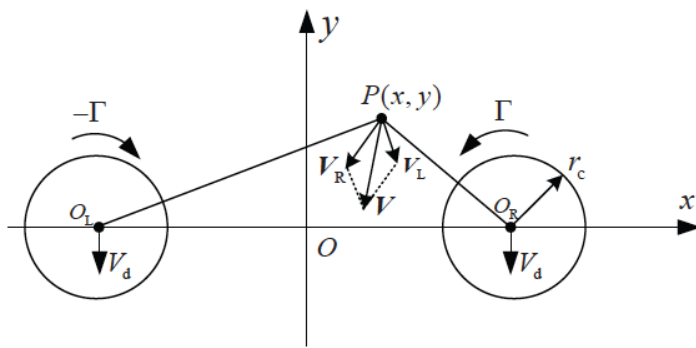
0.5mm -  
4.0 mm

A. B. Kostinski and  
R. A. Shaw, 2009

### Hallock-Burnham model

$$V_{\theta}(r) = \frac{\Gamma_0}{2\pi r} \cdot \frac{r^2}{r^2 + r_c^2}$$

### Biot-Savart Law



$$\mathbf{u}(x, y) = V_L + V_R$$

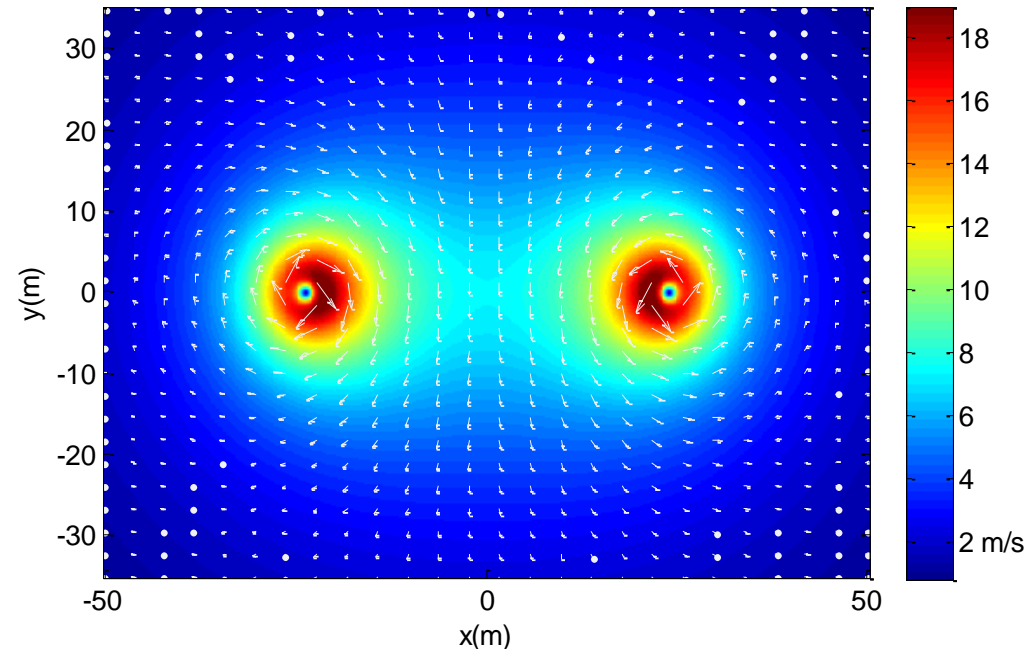
### Descent velocity

$$V_d = \frac{\Gamma_0}{2\pi b_0}$$

### Assumptions for wake vortex:

- ✓ the background atmosphere is still air
- ✓ the wake vortex is in stable phase

### 2D velocity field of A340 wake vortices



Aircraft landing weight: 259000 kg; Landing speed: 290 km/h; Wingspan: 60.30 m

Vertical velocity profile on a line passing through the wake vortex centroids of three types of aircrafts: an A320, an A340 and an A380

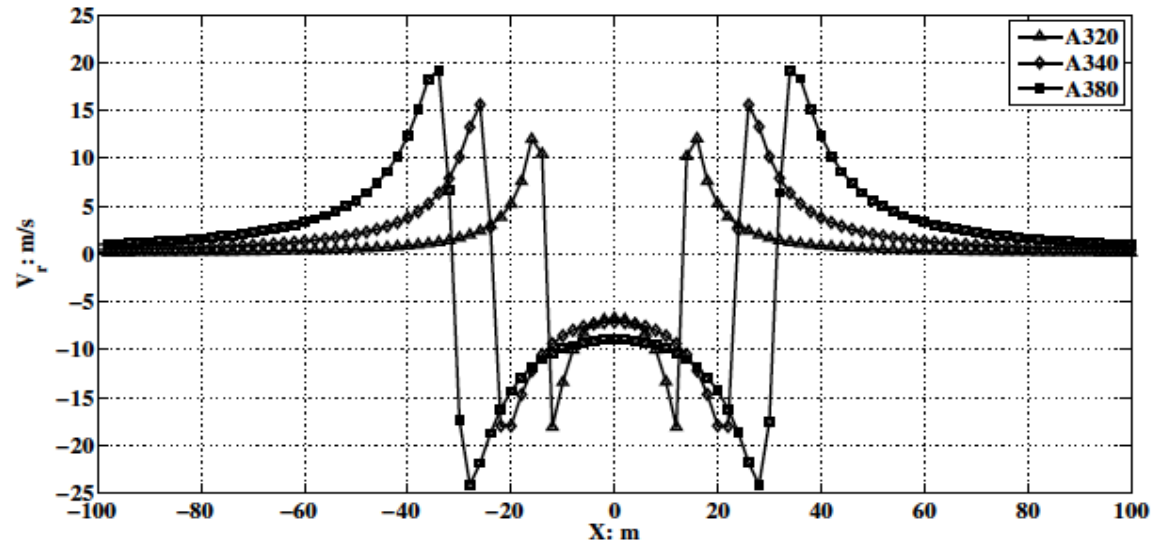
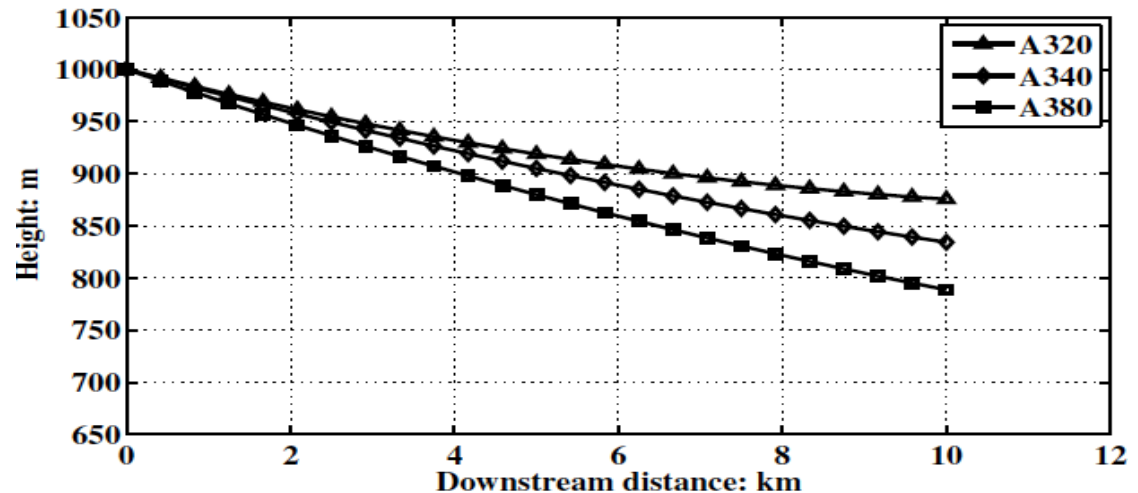


Illustration of the descent of wake vortex pairs behind three types of aircrafts: A320, A340 and A380



### Stokes number

$$S_t = t_s / t_{flow}$$

$$t_s = V_T / g$$

$$t_{flow1} = 2\pi r_{max} / V_{max}$$

$S_t$  characterizes in which extent the particle follows the streamlines of the flow:

- If  $S_t \gg 1$ , the particle's motion is weakly affected by the flow;
- If  $S_t \sim 1$ , the particle's motion is substantially modified by the flow;
- if  $S_t \ll 1$ , the particle's motion approximately follows the flow.

### The Stokes number of raindrops in wake vortex

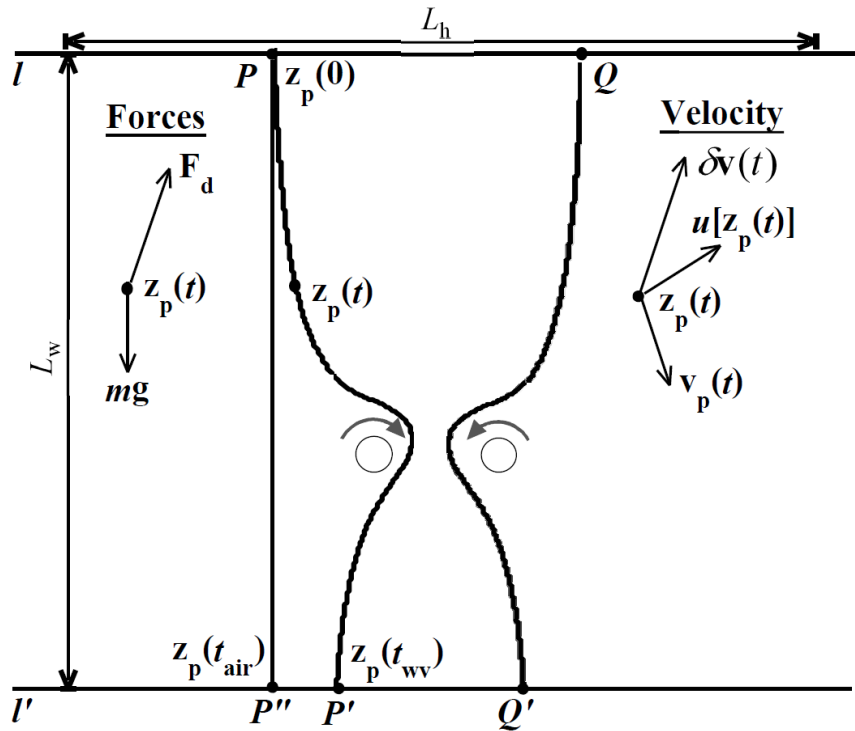
Diameter	Stokes number
0.5 mm	0.2863
1.0 mm	0.5667
2.0 mm	0.9282
4.0 mm	1.2355

As for the raindrops usually encountered during rainfall (0.5 mm - 4 mm),  $S_t \sim 1$ , the trajectories will significantly differ from the streamlines and also from the free fall in still air.

To obtain those trajectories, the computation of the equation of motion applied to the raindrops is thus required.

**Under the assumption of one-way coupling, the motion of a raindrop is governed by**

- ✓ its gravity
- ✓ the fluid drag force



Equation of motion of raindrops

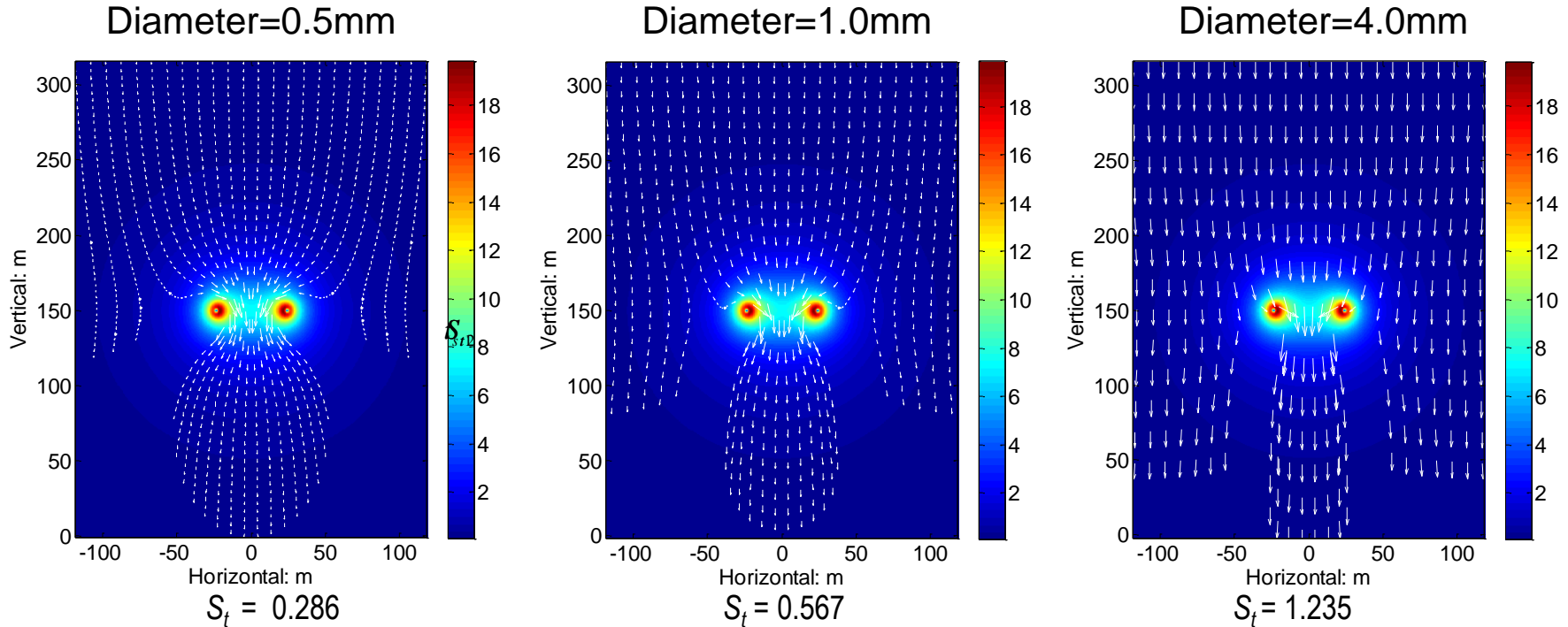
$$\begin{cases} \mathbf{a}(t) = \mathbf{g} + \frac{g}{V_T^2} |\delta \mathbf{v}| \delta \mathbf{v} \\ \frac{d\mathbf{v}_p(t)}{dt} = \mathbf{a}(t) \\ \frac{dz_p(t)}{dt} = v_p(t) \end{cases}$$

$$\delta \mathbf{v} = \mathbf{u}[z_p(t)] - \mathbf{v}_p(t)$$

Four variables differential equations

$$\begin{cases} \frac{dx_p}{dt} = v_x \\ \frac{dy_p}{dt} = v_y \\ \frac{dv_x}{dt} = \frac{g}{V_T^2} |\delta \mathbf{v}| [u_x(x_p, y_p) - v_x] \\ \frac{dv_y}{dt} = -g + \frac{g}{V_T^2} |\delta \mathbf{v}| [u_y(x_p, y_p) - v_y] \end{cases}$$

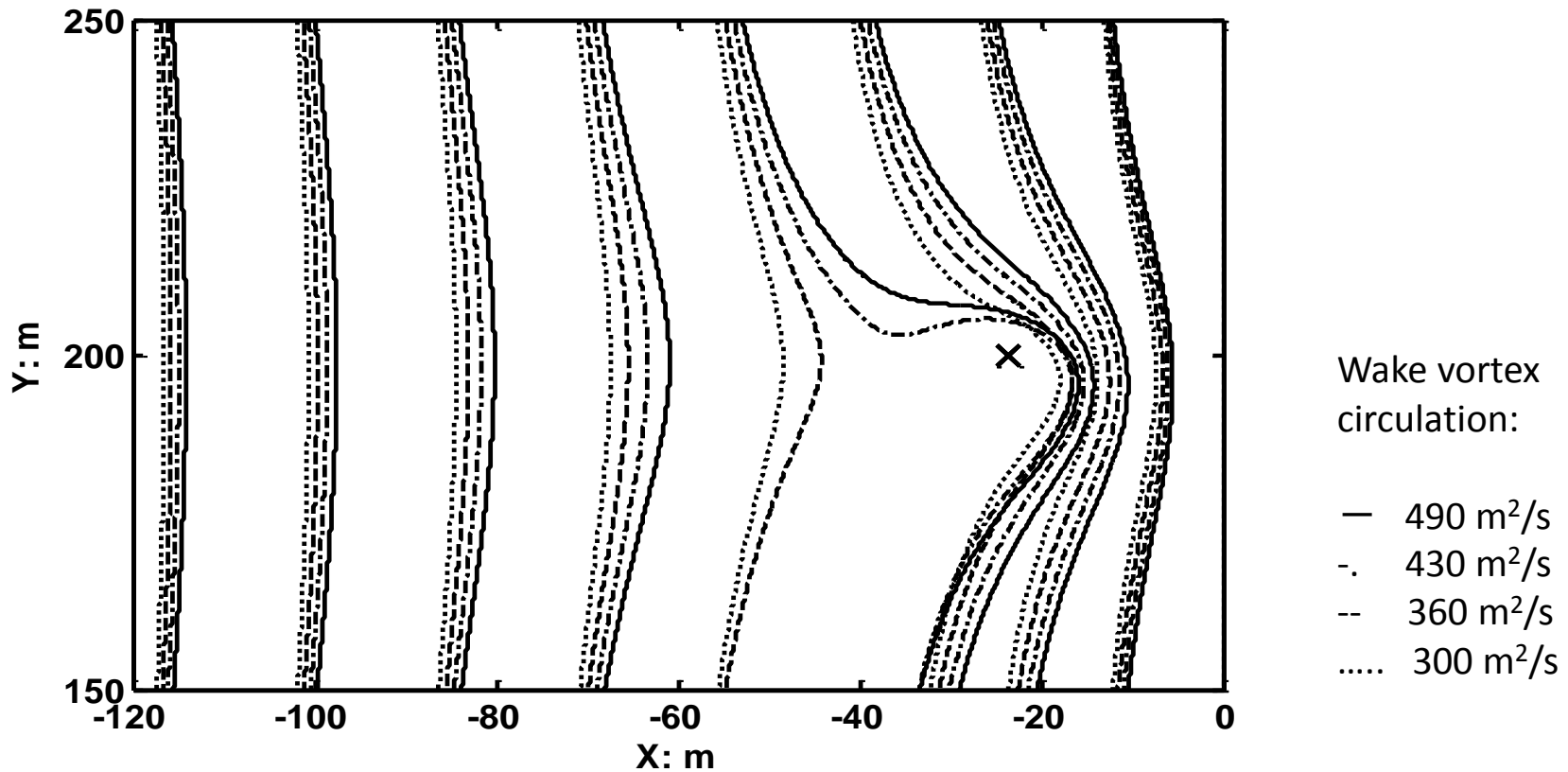
**4<sup>th</sup> order four variables Runge-Kutta algorithm**



- The trajectories of raindrops with smaller diameters seem to be more largely changed by the vortex flow;
- In some part of the region under the vortex flow, there are no raindrops falling down;
- In the region between the two vortex cores, some of raindrops are preferentially concentrated, the velocities of the raindrops here are also considerably increased.

### Raindrops' trajectories in wake vortices with different circulation

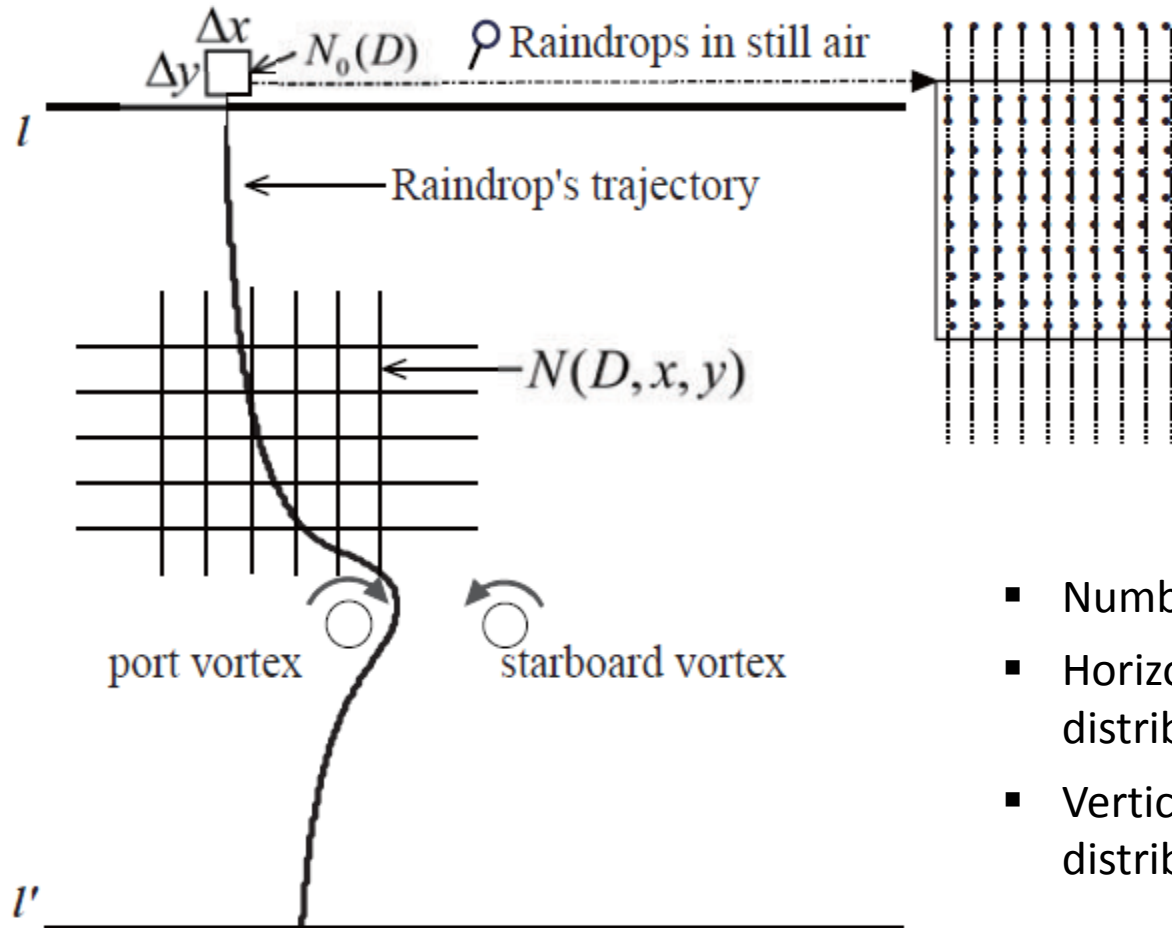
$D = 1.0 \text{ mm}$



The motion characteristic of raindrops in wake vortices is representative of the vortex strength.



The methodology to approximately compute raindrops' distribution in wake vortices by box counting method:

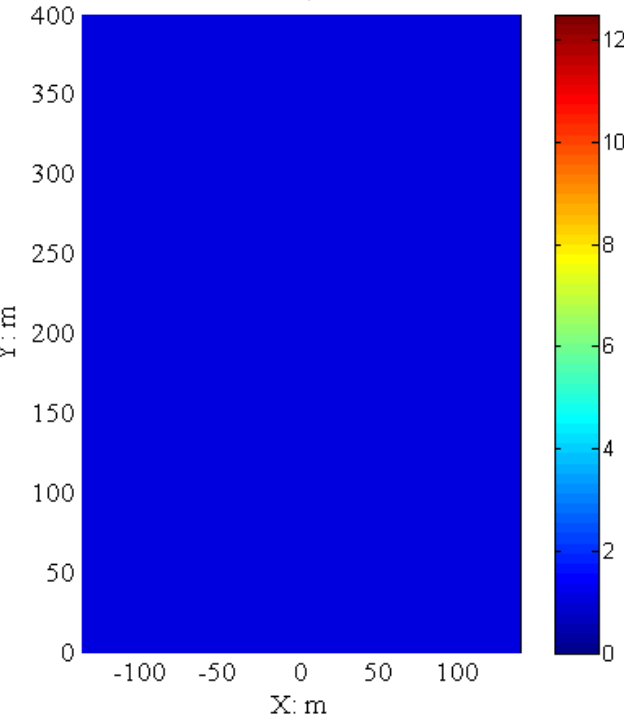


- Number concentration
- Horizontal velocity distribution
- Vertical velocity distribution

In the wake vortex region, there are two columns where the raindrops' concentration is zero and between these two columns, there are two narrow regions where the number concentration of raindrops is enhanced.

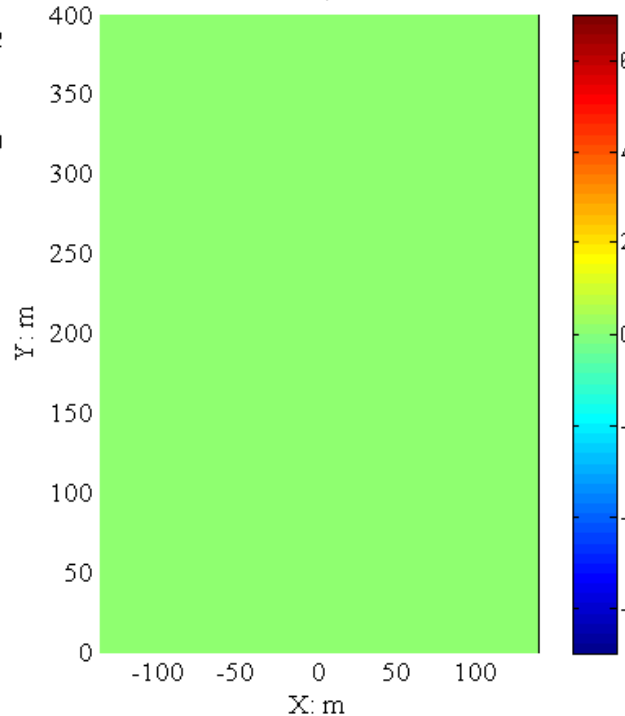
**Number concentration**

D: 1 mm, t = 0 s



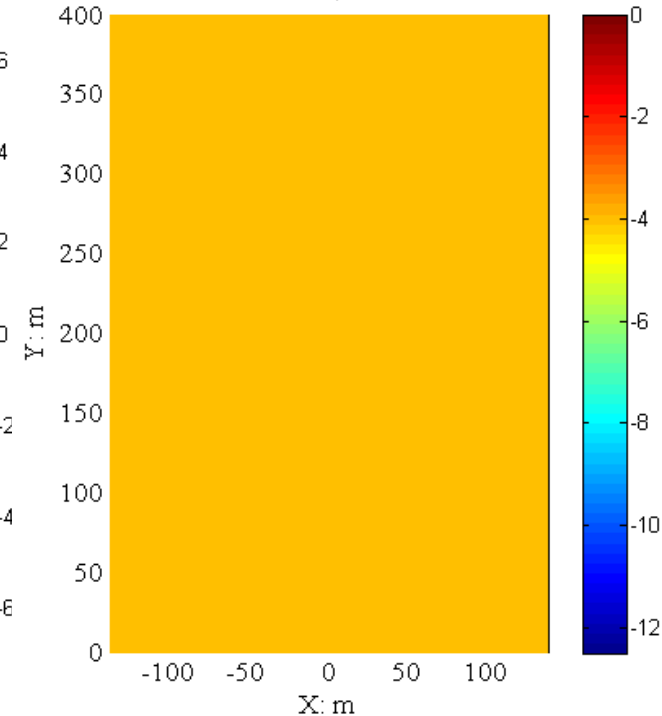
**Horizontal velocity (m/s)**

D: 1 mm, t = 0 s

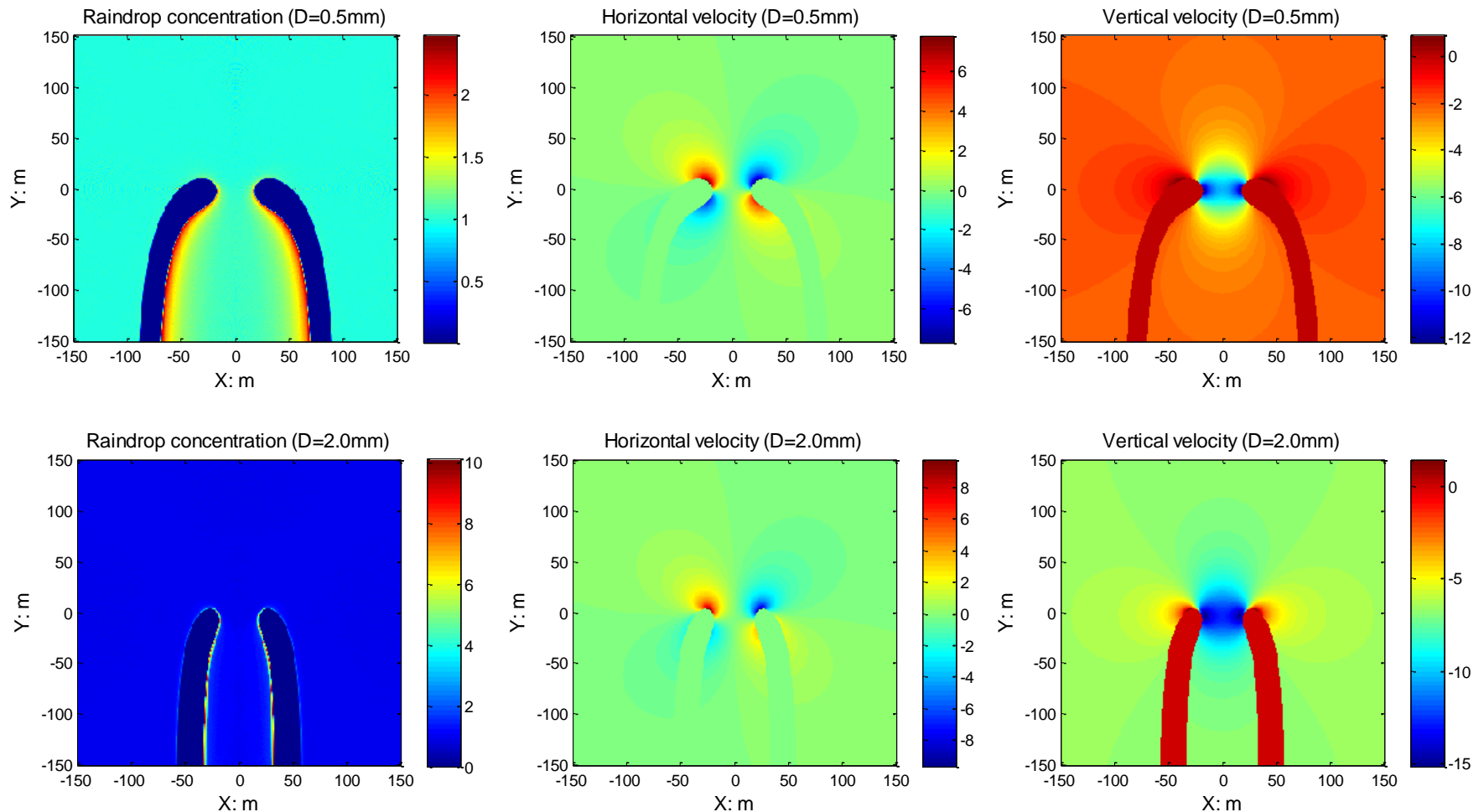


**Vertical velocity (m/s)**

D: 1 mm, t = 0 s



Raindrops' number concentration and velocity distribution (0.5mm, 2 mm)





## 3. Radar signatures simulation

- 3.1 Wake vortex Radar simulators
- 3.2 X band Radar in staring mode
- 3.3 X band Radar in scanning mode
- 3.4 W band Radar in scanning mode

### Microwave properties of raindrops

#### Rayleigh Approximation

✓ S, C, X bands

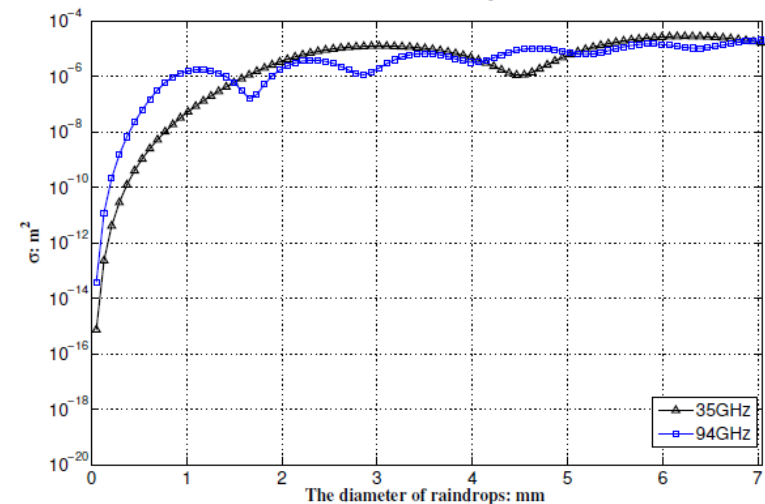
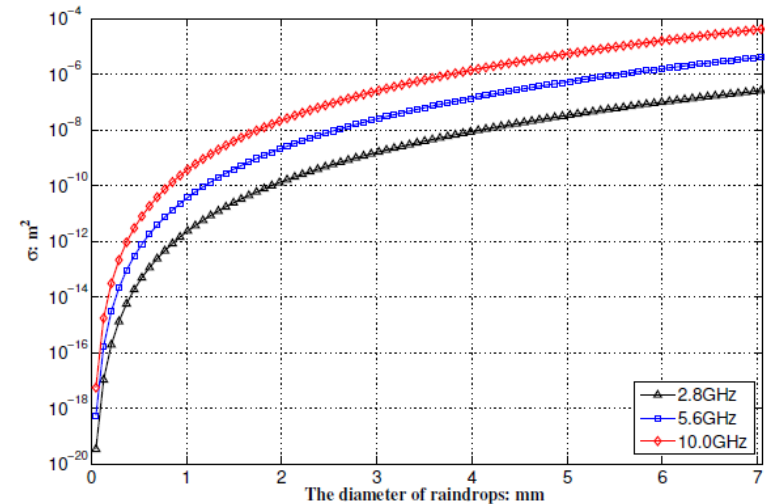
$$\sigma = \frac{\pi^5}{\lambda^4} |K|^2 D^6, K = \frac{m^2 - 1}{m^2 + 2}$$

#### Mie Formulas

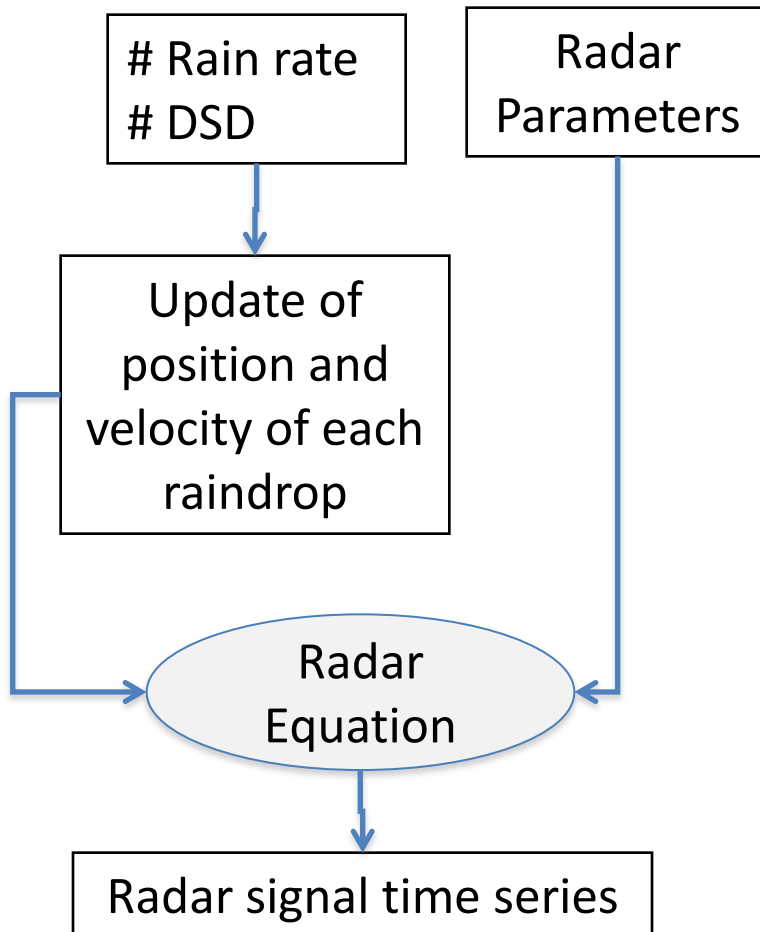
✓ Ka, W bands

$$\sigma = \frac{\lambda^2}{4\pi} \left| \sum_{n=1}^{\infty} (-1)^n (2n+1) (a_n - b_n) \right|^2$$

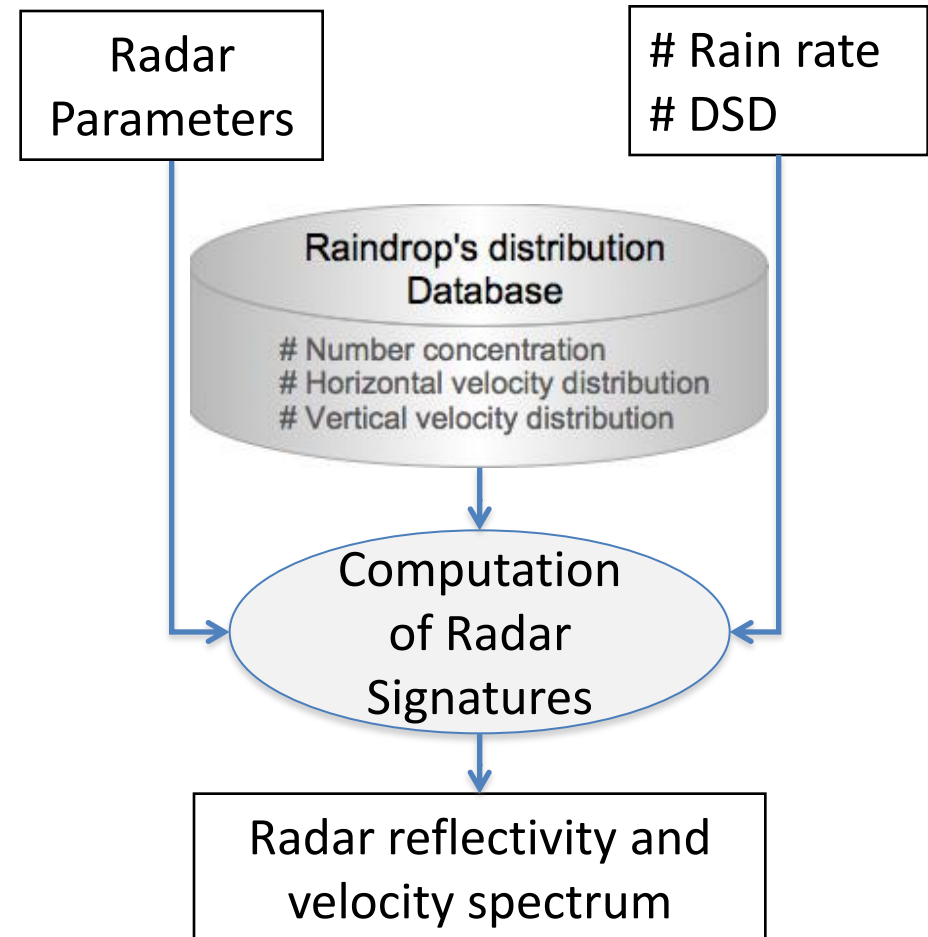
### Raindrops' RCS as function of diameter



### Simulator A:



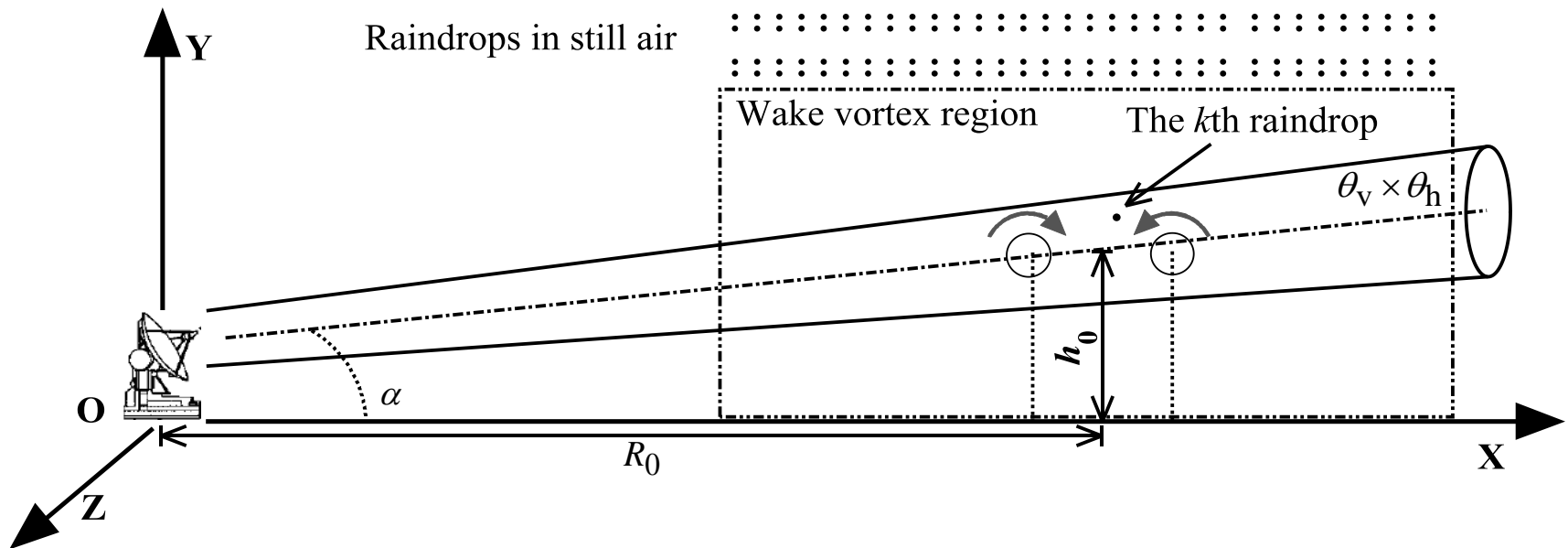
### Simulator B:



**Simulator A**: A time series wake vortex radar simulator

$$s_k(n) = A_k \exp \left[ -j2\pi f_c \frac{2(r_k + nTv_k)}{c} \right] \quad A_k = H \frac{\sqrt{\sigma_k}}{r_k^2} w_a(\alpha_k, \phi_k) w_r(r_k), \quad H = \sqrt{\frac{P_t G^2 \lambda^2}{(4\pi)^3 L}}$$

$$S_r(n) = \sum_{k=1}^{N_r} s_k(n) + n_s$$



### Simulator B : Raindrop's distribution based radar simulator

The radar reflectivity of raindrops in the  $k$ th radar cell is given by

$$\eta_k = \frac{1}{V_k} \sum_{D=D_{\min}}^{D_{\max}} \sigma(D)N(D)\Delta D \int_{i,j} \eta_N(D, i, j)$$

where  $i, j$  are indices of the grid boxes which are located in the  $k$ th radar cell.

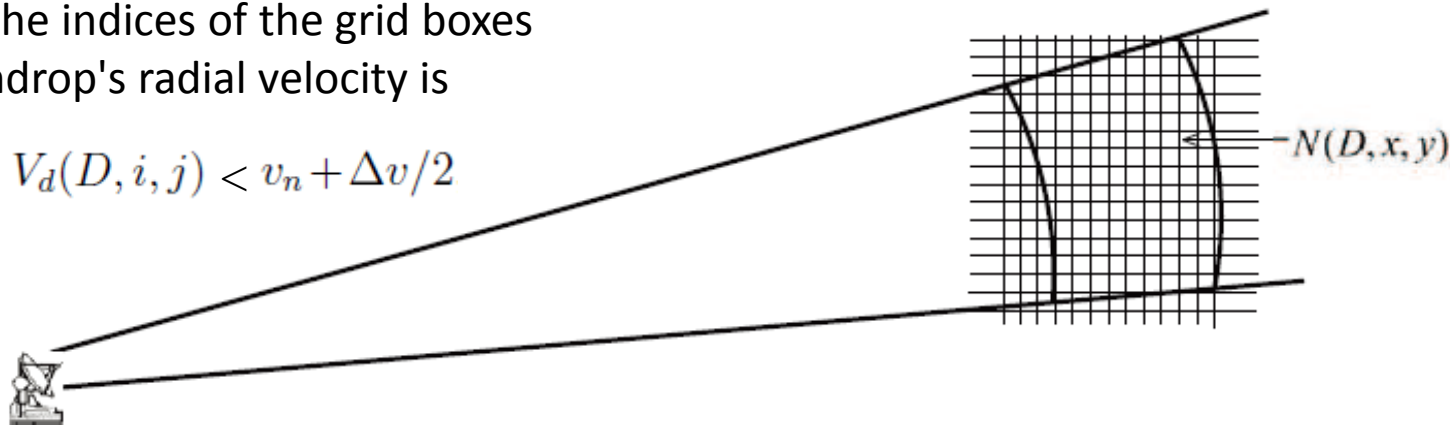
The magnitude of Doppler velocity spectrum  $S(r_k, v_n)$  is the sum of returned power from all the raindrops in the  $k$ th radar cell with the same radial velocity

$$S(r_k, v_n) = \frac{P_t G^2 \lambda^2 N_p^2}{(4\pi)^3 r_k^4 L} \sum_{D=D_{\min}}^{D_{\max}} \sigma(D)N(D)\Delta D \int_{i,j} \eta_N(D, i, j)$$

where  $i, j$  are the indices of the grid boxes

where the raindrop's radial velocity is

$$v_n - \Delta v/2 \leq V_d(D, i, j) < v_n + \Delta v/2$$





### Simulator A:

Radar signatures simulation based on superimposing the radar signals from all the raindrops in the radar cell

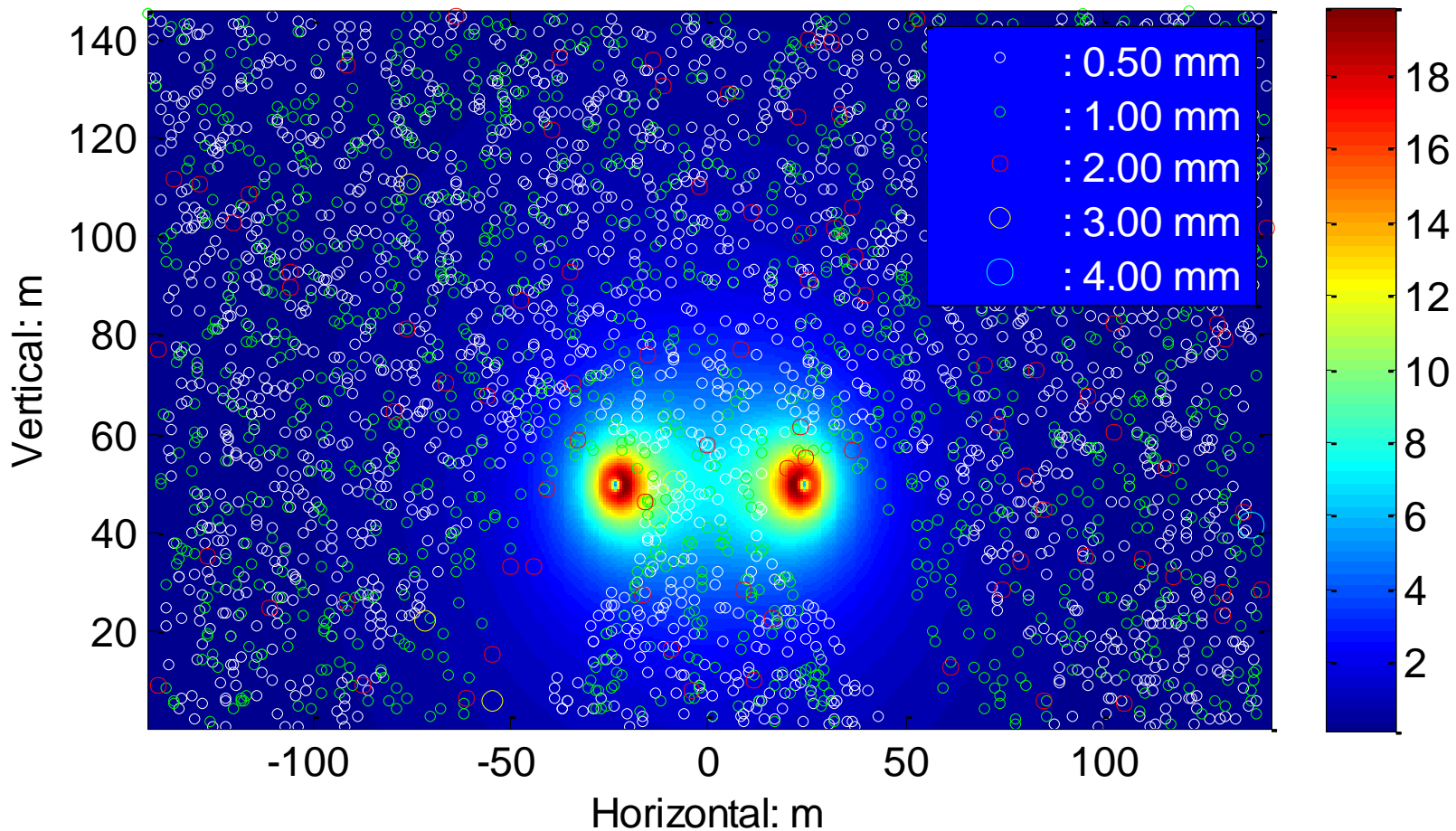
### Simulator B:

Radar signatures simulation based on the raindrops' statistical distribution

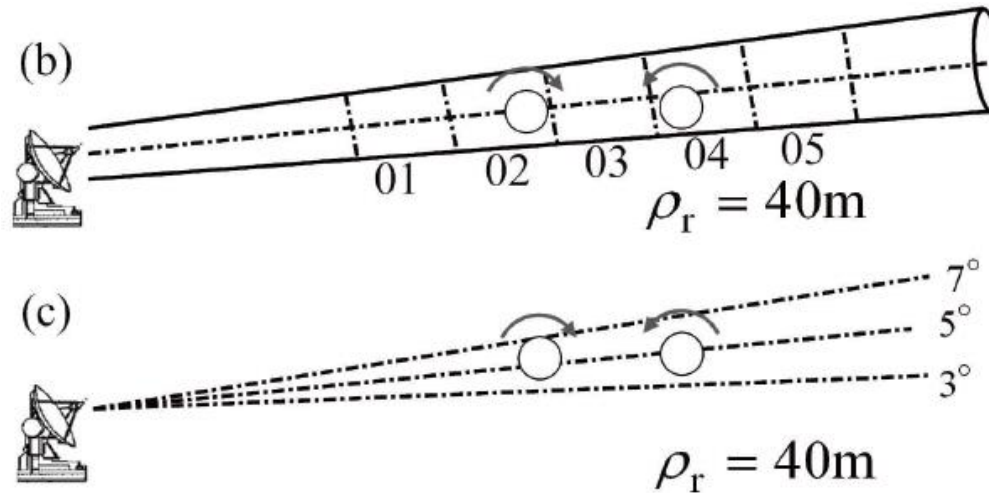
- Firstly, the database of the raindrop's distribution is independent of the rain rate and DSD model, the radar signatures of raindrops in wake vortices under different rain rates or DSD models can be simulated very easily and efficiently.
- Secondly, the computation load is much lower compared to the simulation based on the generation a large population of raindrops in the radar resolution volume.
- Thirdly, the in-phase (I) and quadrature (Q) components of the radar signal time series can also be obtained by taking an inverse discrete Fourier transform of the spectrum and noise model.

### Generation of the initial raindrops

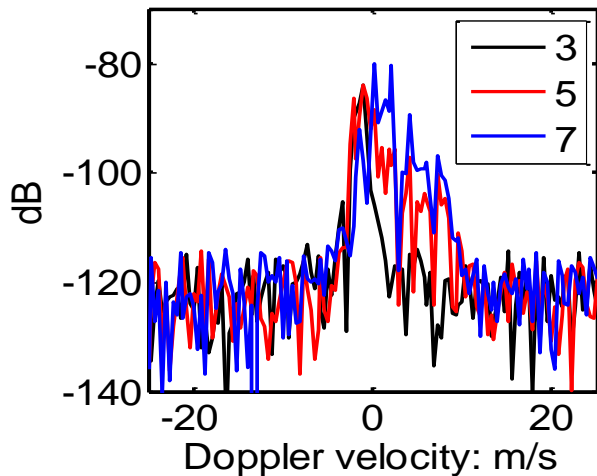
Rainrate: 1.19 mm/h



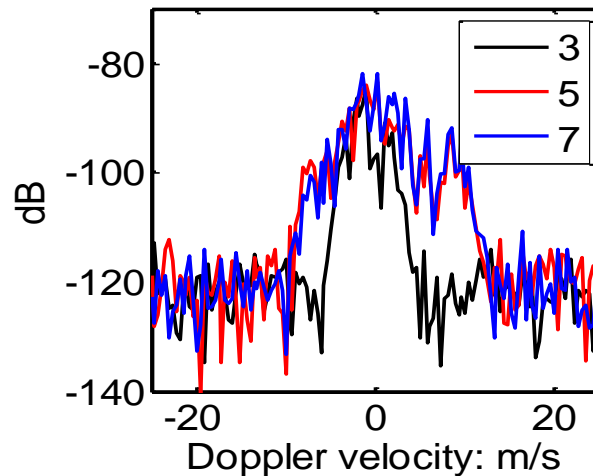
### Doppler spectrum for 40m radial resolution



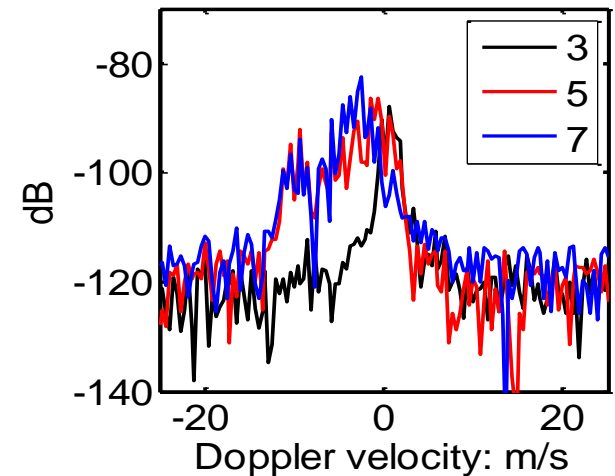
Radar cell: 02



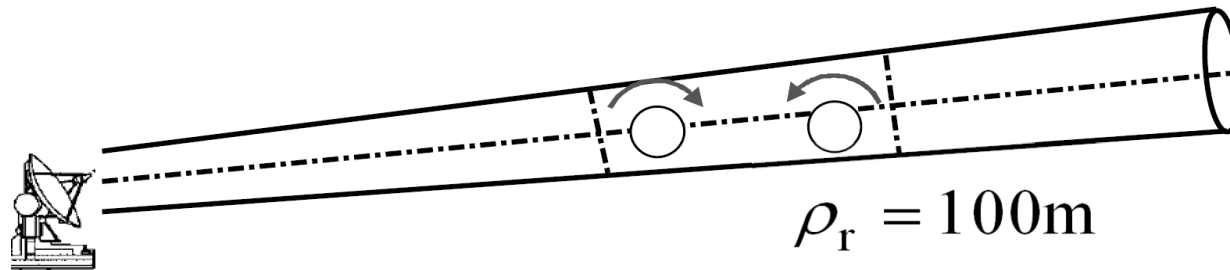
Radar cell: 03



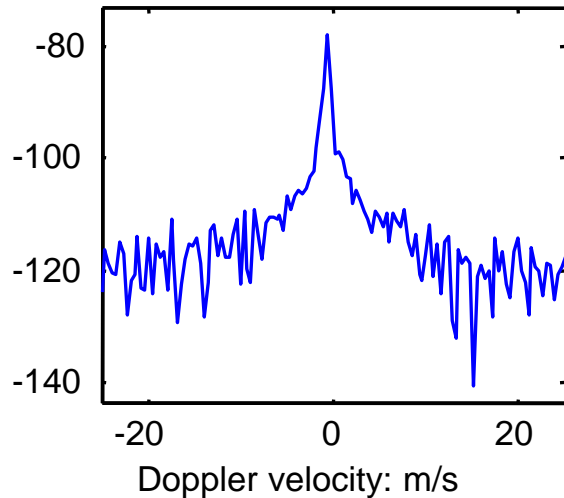
Radar cell: 04



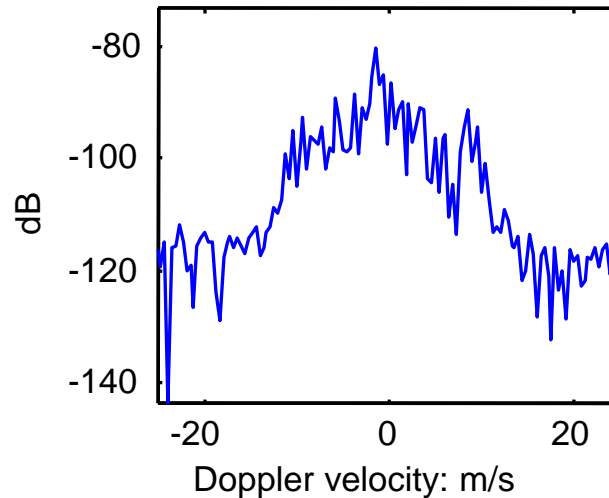
### Doppler spectrum for 100m radial resolution



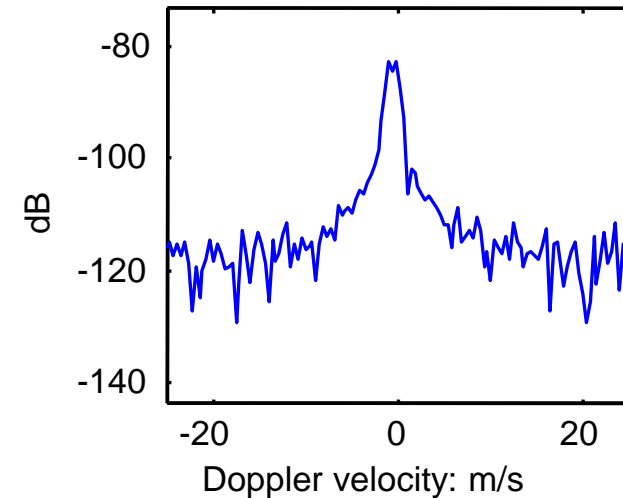
Radar cell: 01



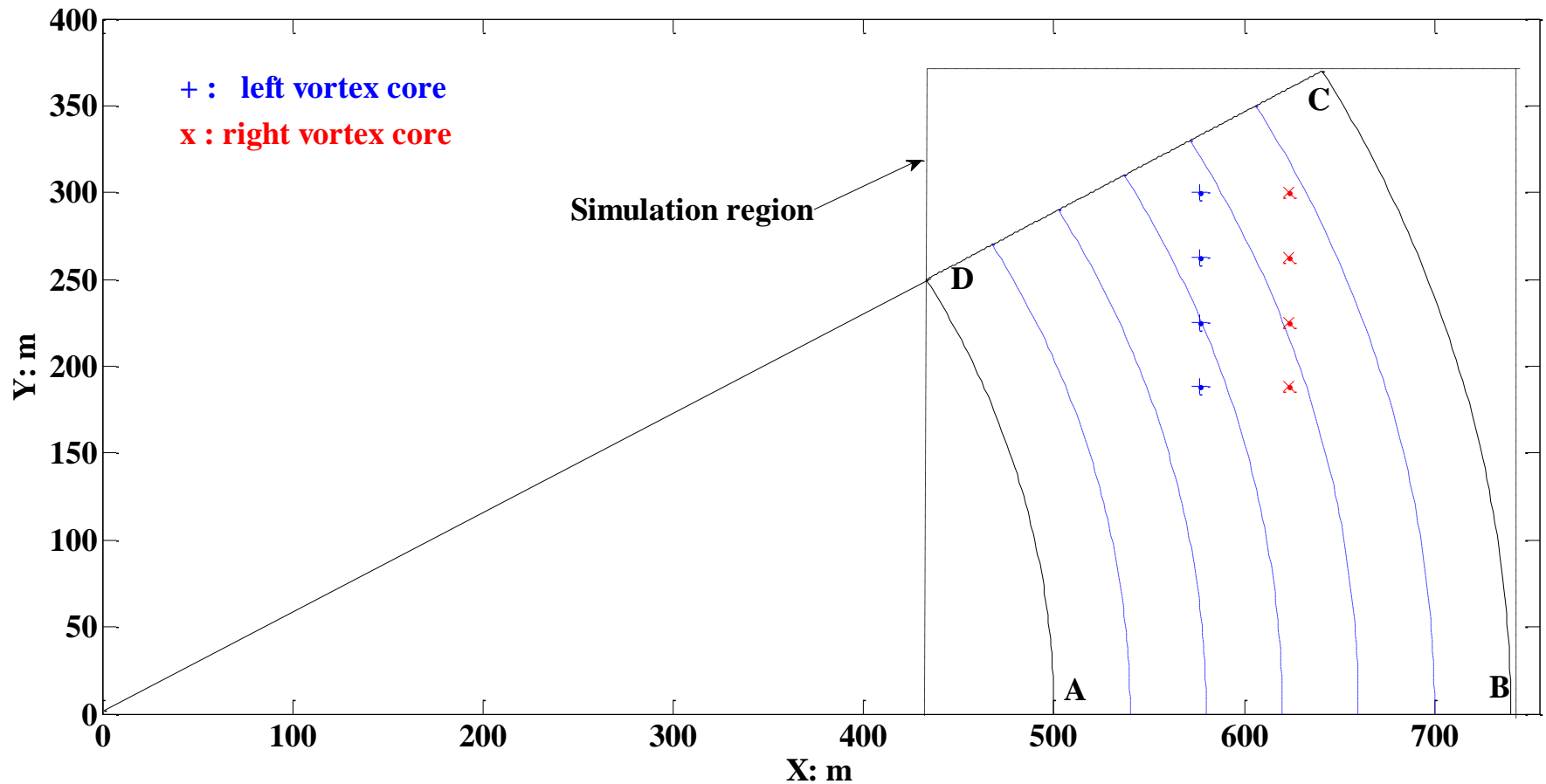
Radar cell: 02



Radar cell: 03

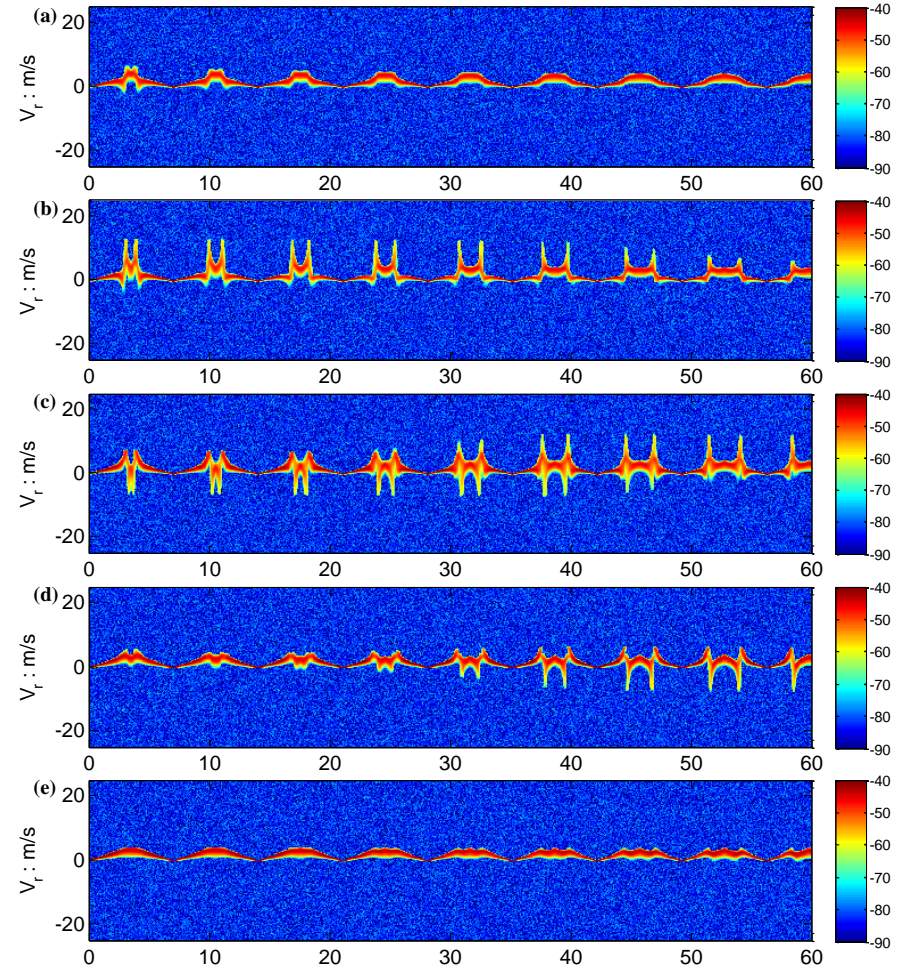
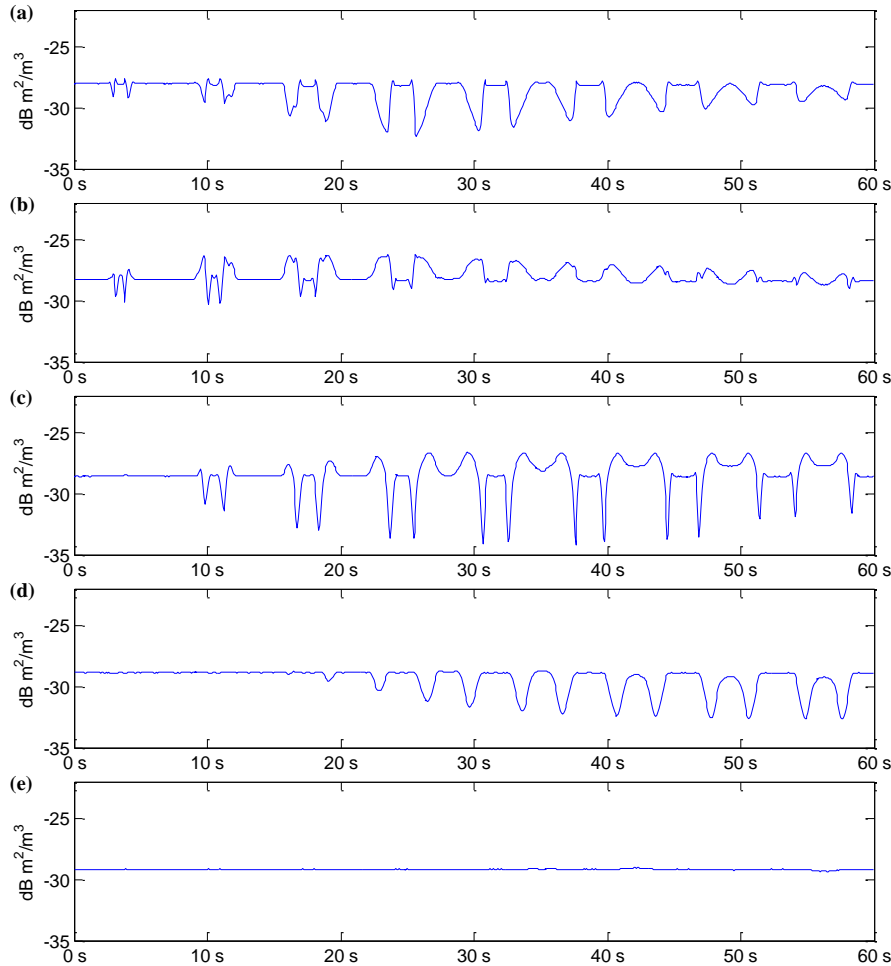


### Radar-Wake vortex geometry configuration (close to runway)

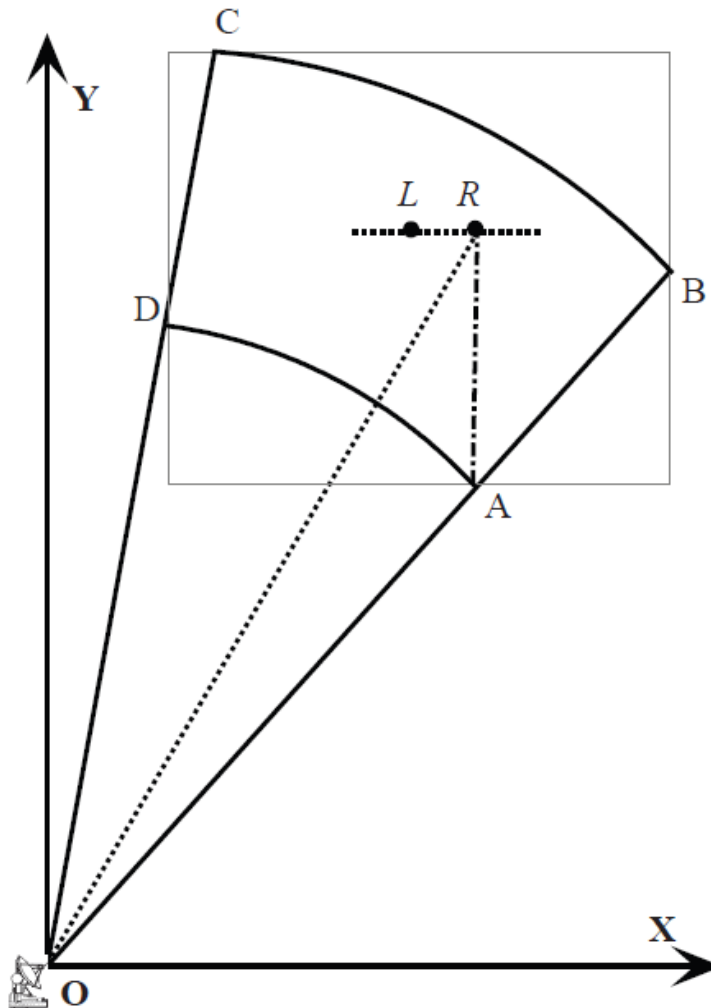


Radar reflectivity (rain rate: 10 mm/h)

Time-Doppler velocity spectrum



### Radar-Wake vortex geometry configuration (Thales radar trials)



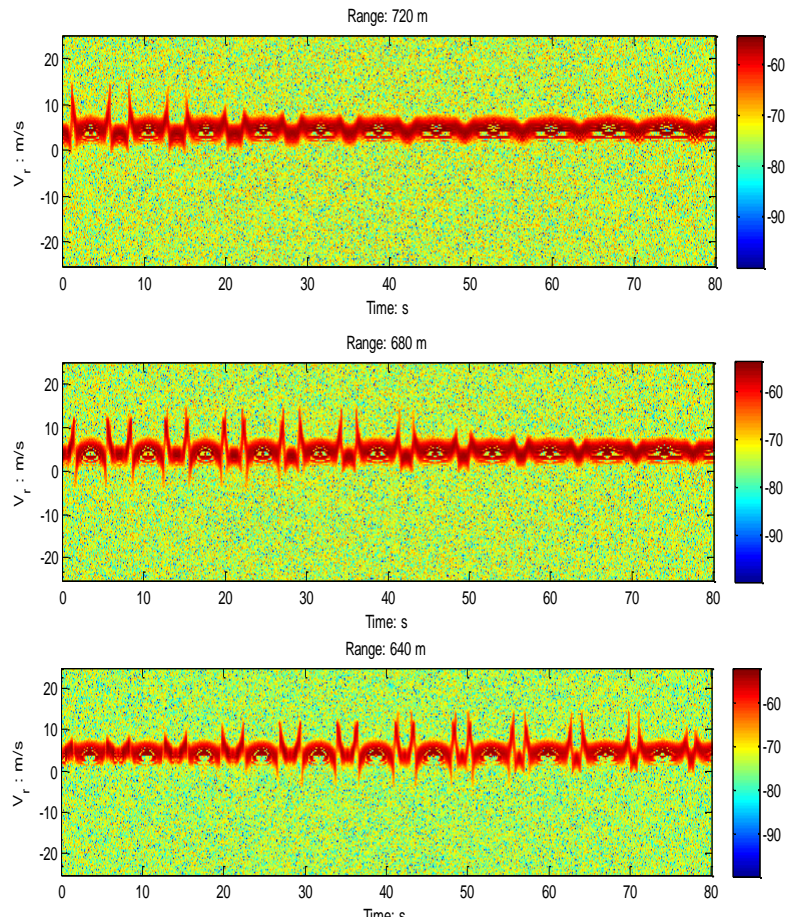
- Scanning rate:  $8^\circ / \text{s}$
- Scanning area:  $50^\circ - 80^\circ$
- Location of the right vortex core: 700 m,  $60^\circ$  (élévation)

$M$  range cells,  $N$  elevation angles

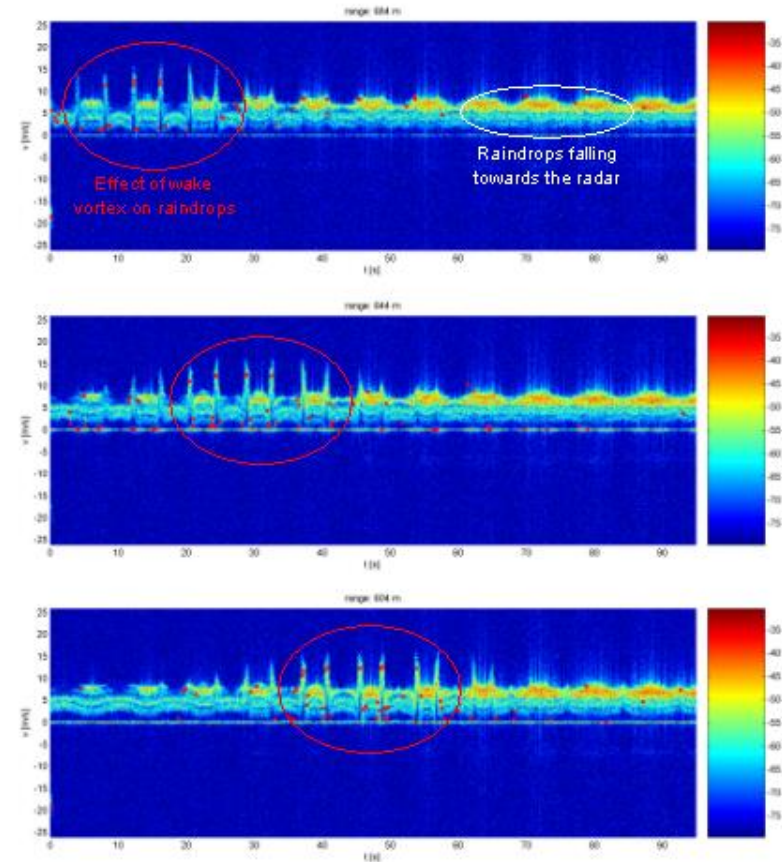
Output: Radar signatures  $M \times N$

For each radar cell, compute the time- Doppler signature in scanning mode

### Comparison with X band radar trials (F. Barbaresco 2012)



(a) Simulated time-Doppler spectrum of raindrops in wake vortices



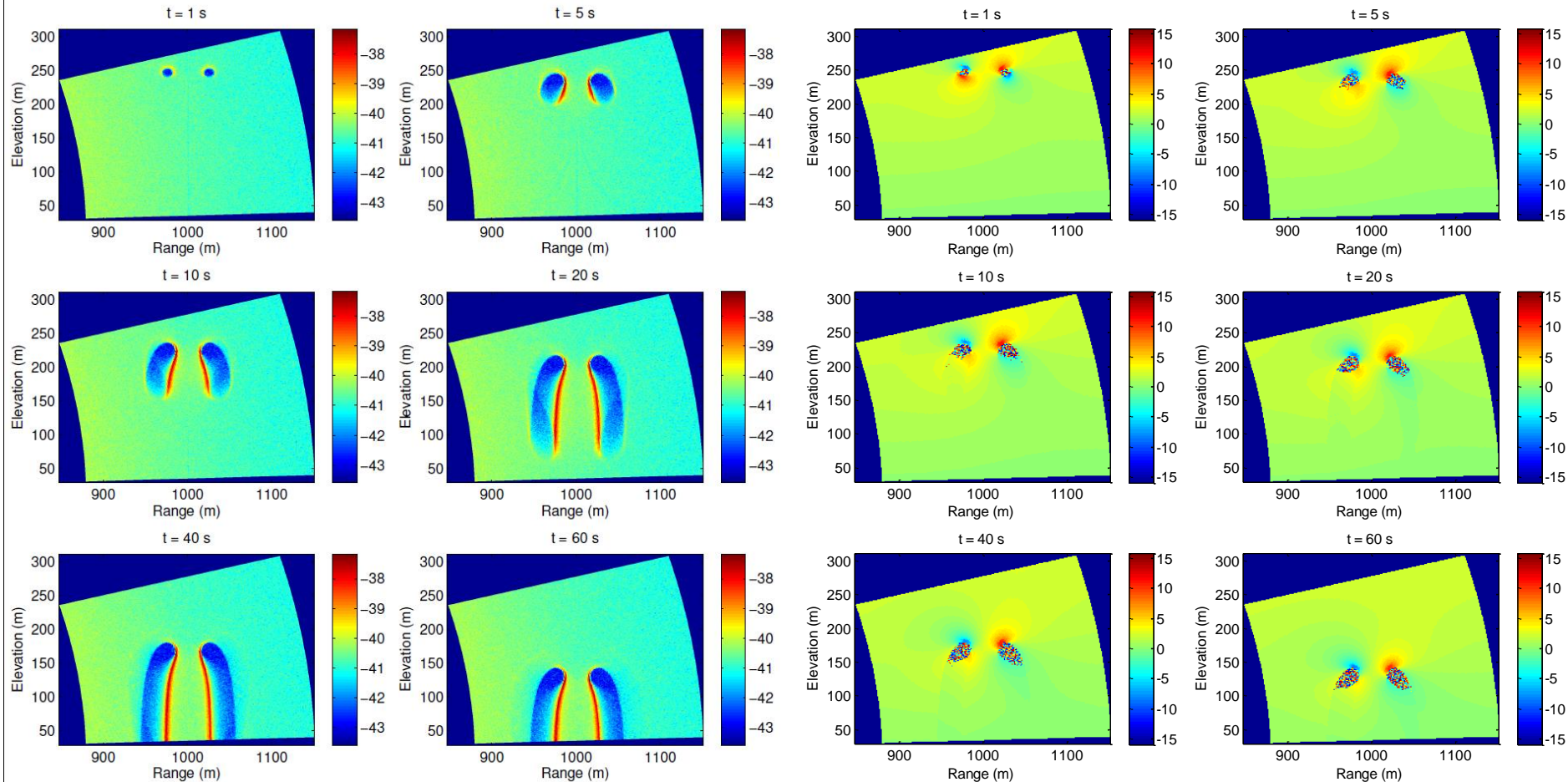
(b) Time-Doppler spectrum observed by Thales radar trials in 2011



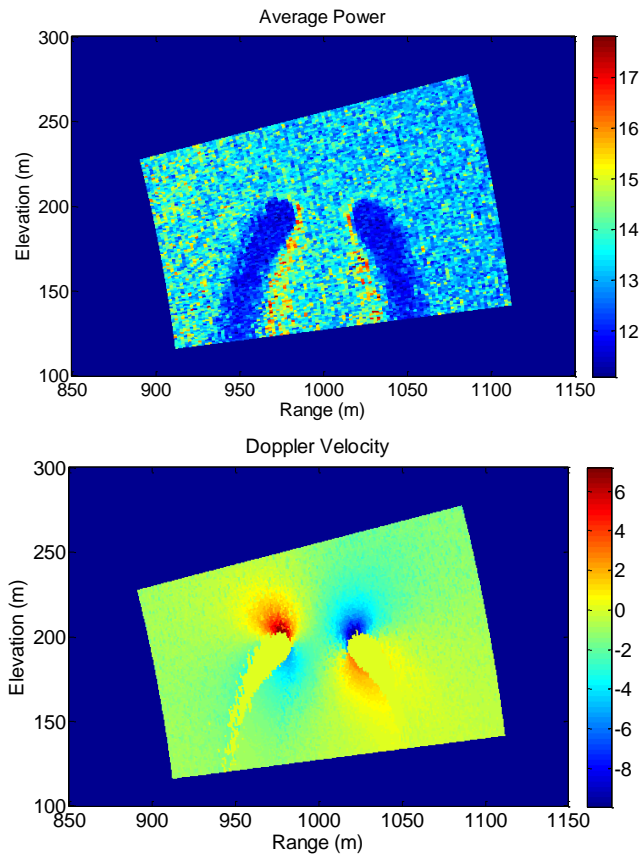
### W band radar signatures of raindrops at different times (rain rate: 2 mm/h)

Average received power

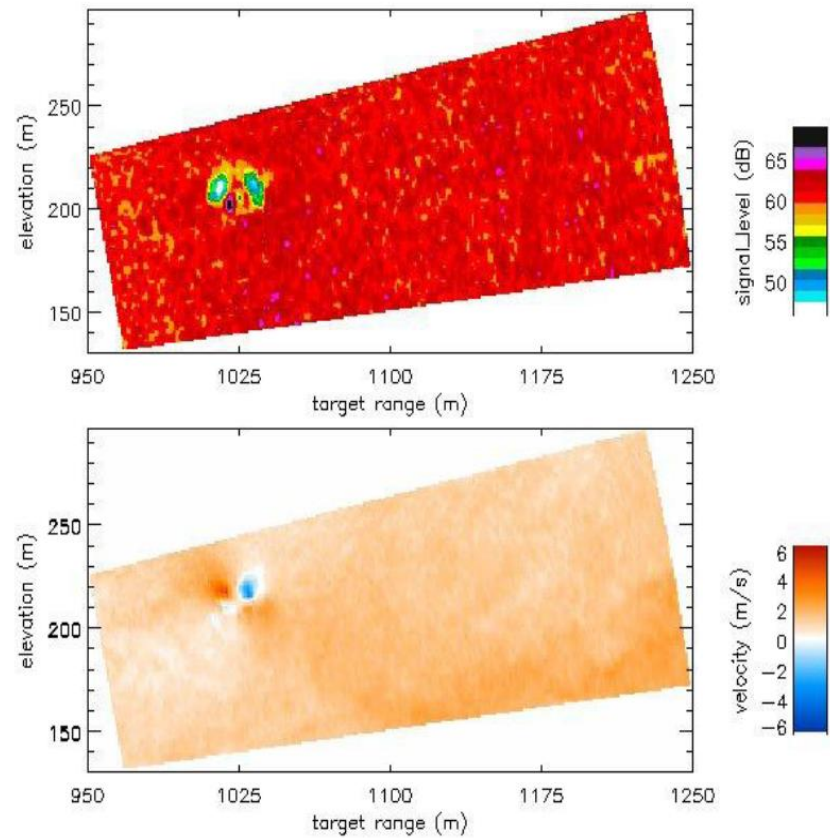
Peak Doppler velocity profile



### Comparison with W band radar trials (T. A. Seliga 2009)



Rain rate 2.0mm/h, Range Resolution: 2 m



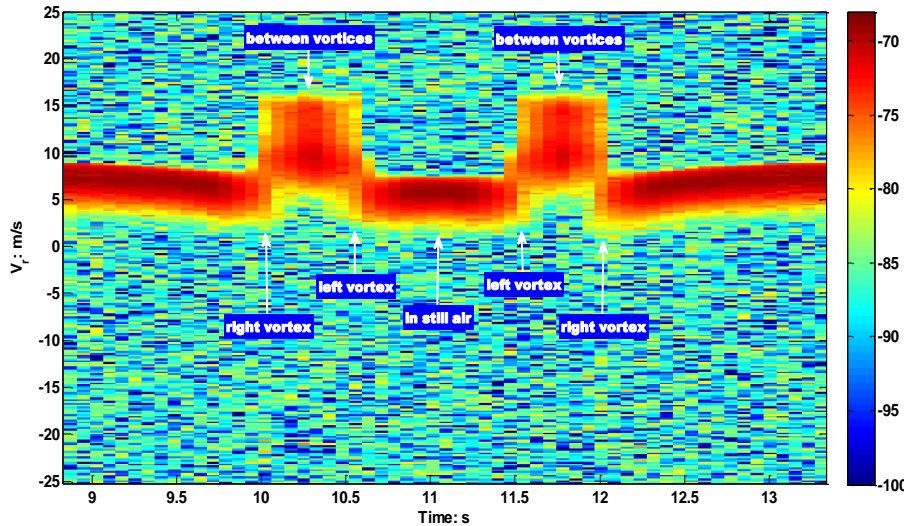
W-Band Radar Measurements (T. A. Seliga 2009)



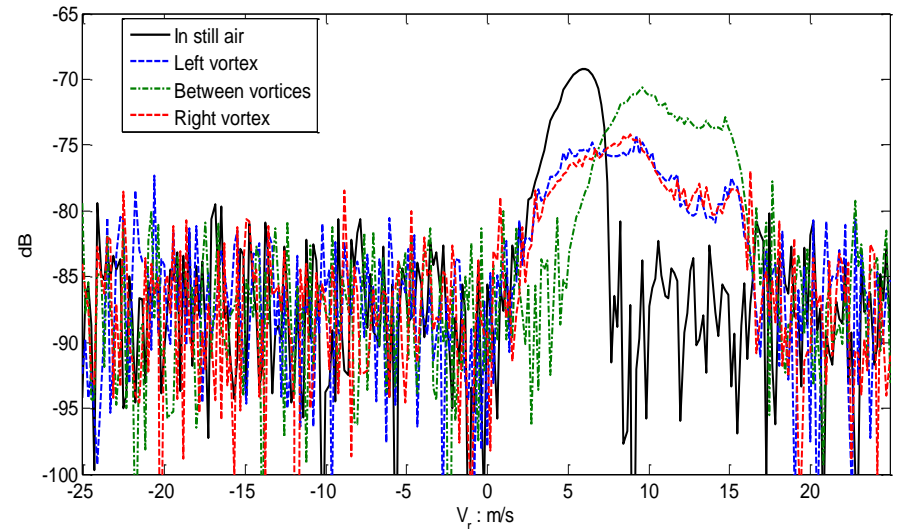
## 4. Radar signatures interpretation

- 4.1 Dependence of radar signatures on vortex circulation
- 4.2 Wake vortex detection
- 4.3 Wake vortex parameter estimation

### X band Radar Doppler signatures in one scanning period



Time-Doppler spectrum of raindrops in one scanning period



Comparison of the Doppler velocity spectrums of raindrops in still air and in wake vortices

- The Doppler spectrums widths of raindrops around the left vortex and right vortex are obviously extended
- The Doppler spectrum of raindrops between the two vortices are shifted and the spectrum widths are also extended

Three moments of radar Doppler spectrum are utilized to interpret the radar signatures:

- radar average received power (zeroth moment),

$$\overline{P_r} = \sum_{n=1}^{N_p} S(r_k, v_n) \cdot \Delta v$$

- mean Doppler velocity (first moment )

$$\overline{S}(r_k, v_n) = \frac{S(r_k, v_n)}{\sum_{n=1}^{N_p} S(r_k, v_n) \cdot \Delta v} = \frac{S(r_k, v_n)}{\overline{P_r}}$$

$$\overline{v_r} = \sum_{n=1}^{N_p} v_n \overline{S}(r_k, v_n) \cdot \Delta v$$

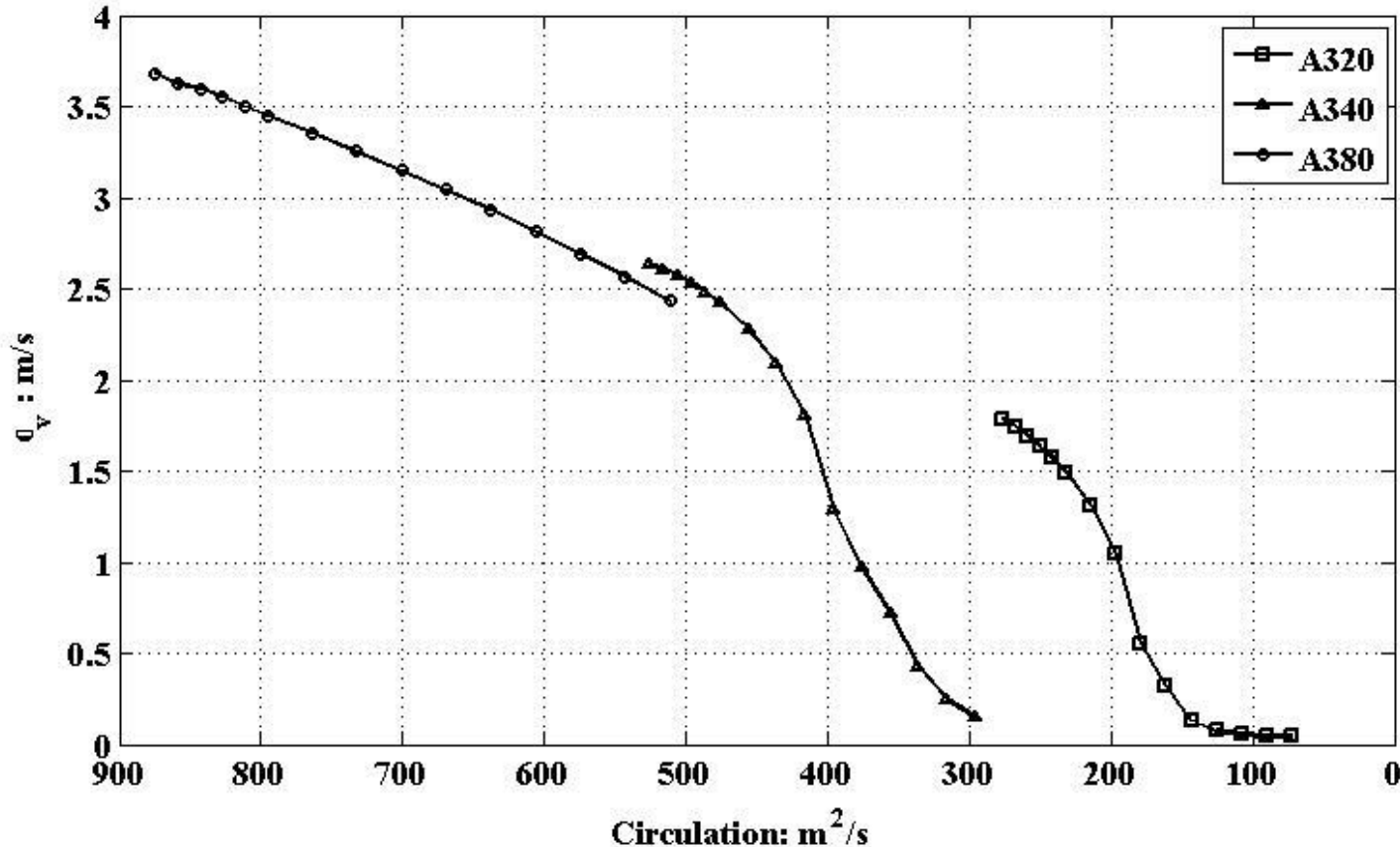
- Doppler spectrum width (second moment )

$$\sigma_v^2 = \sum_{n=1}^{N_p} (v_n - \overline{v_r})^2 \overline{S}(r_k, v_n) \cdot \Delta v$$

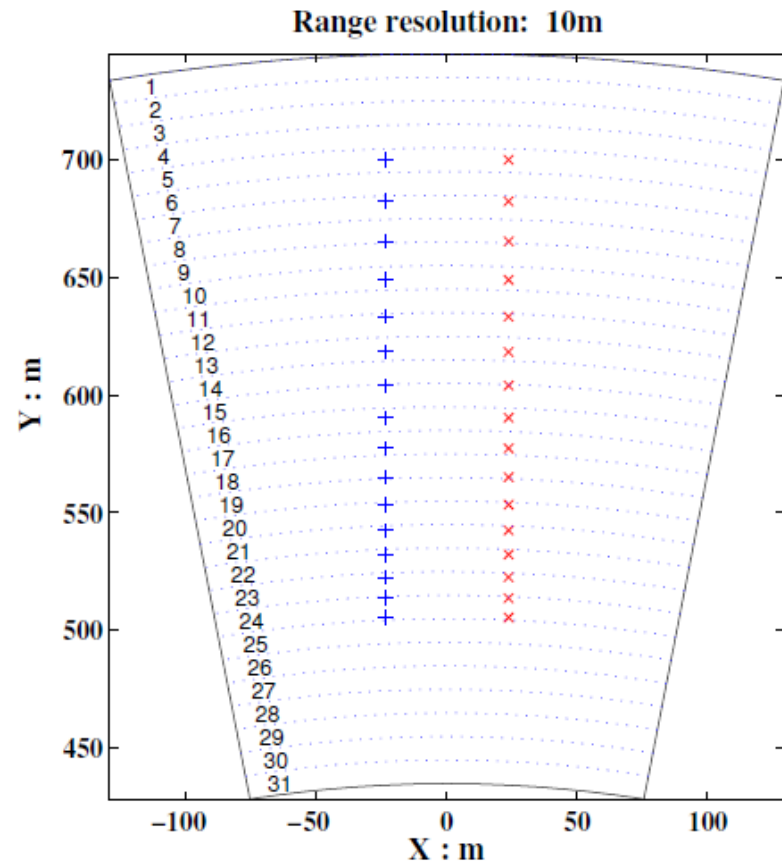
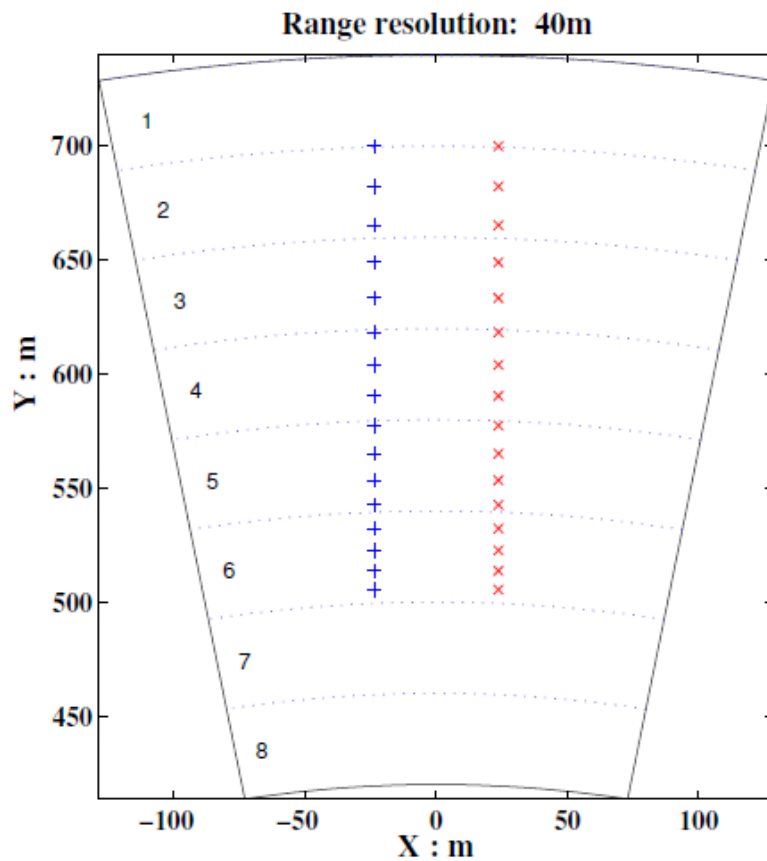
Obviously, the mean Doppler velocity is related to the power weighted mean radial motion of the particles and the Doppler spectrum width is related to the relative particle motions.

### Relationship between Doppler spectrum width of raindrops and vortex circulation

The Doppler spectrum width of raindrops is representative of wake vortex circulation, as vortex circulation decays, the Doppler spectrum width of raindrops is decreasing.

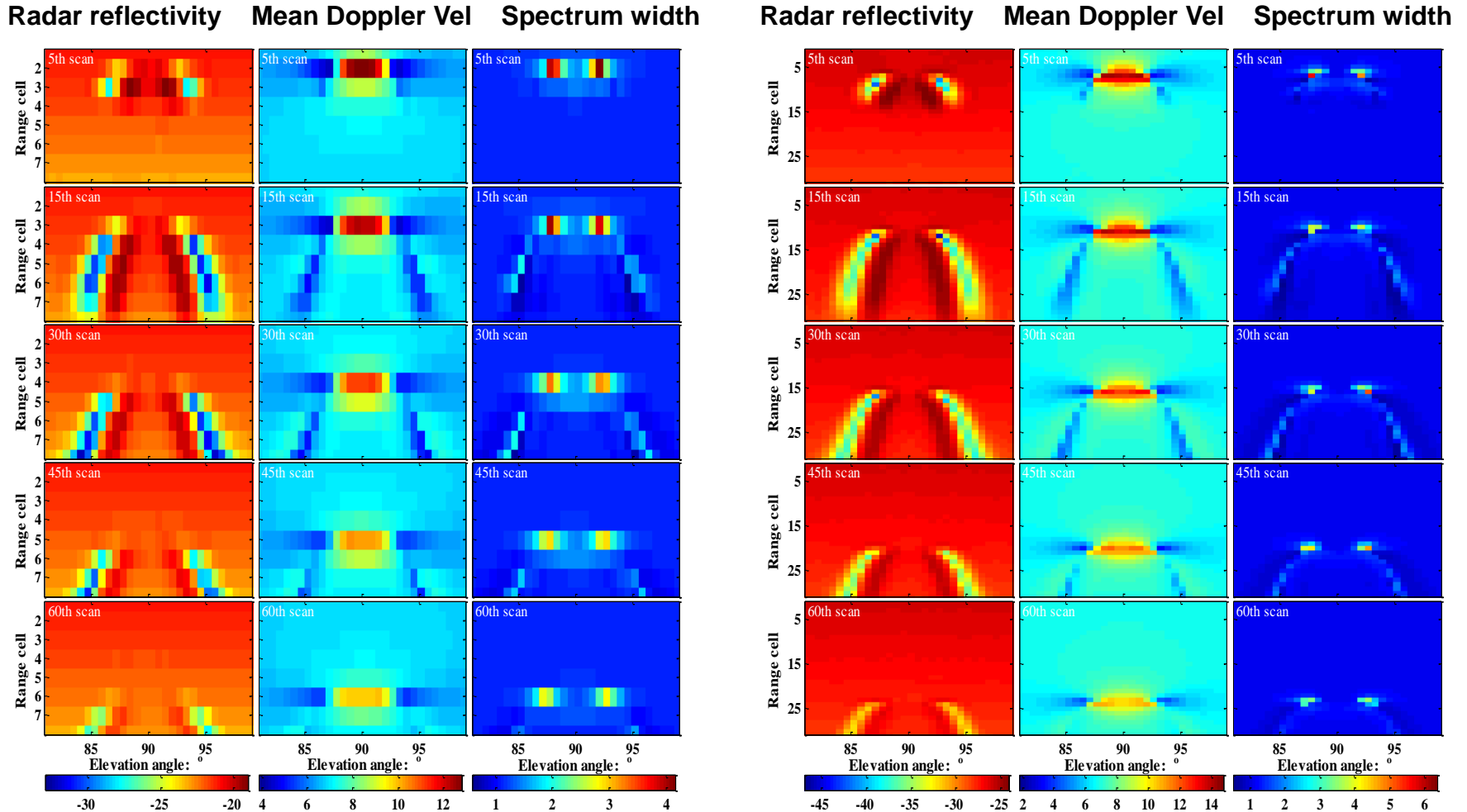


### Radar geometry configurations for different radar range resolutions



'+' and 'x' indicate the location of the left and right vortex respectively

### Interpretation of radar Doppler signatures of raindrops

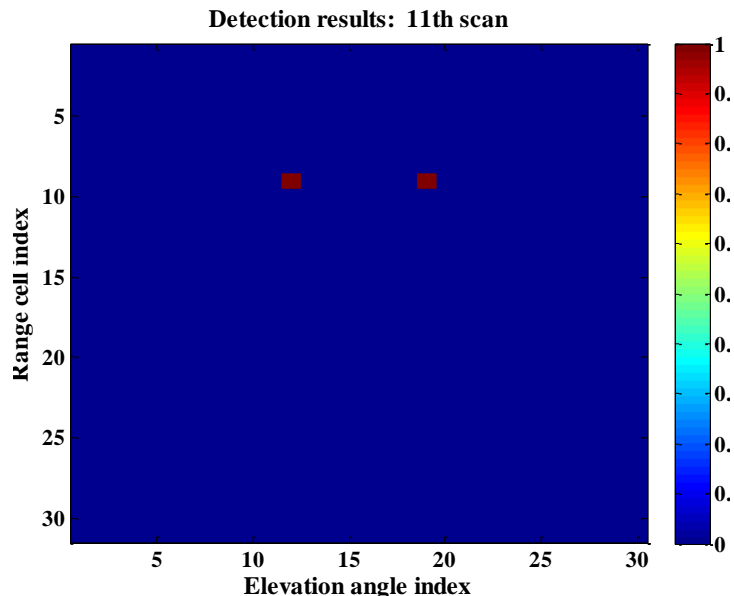
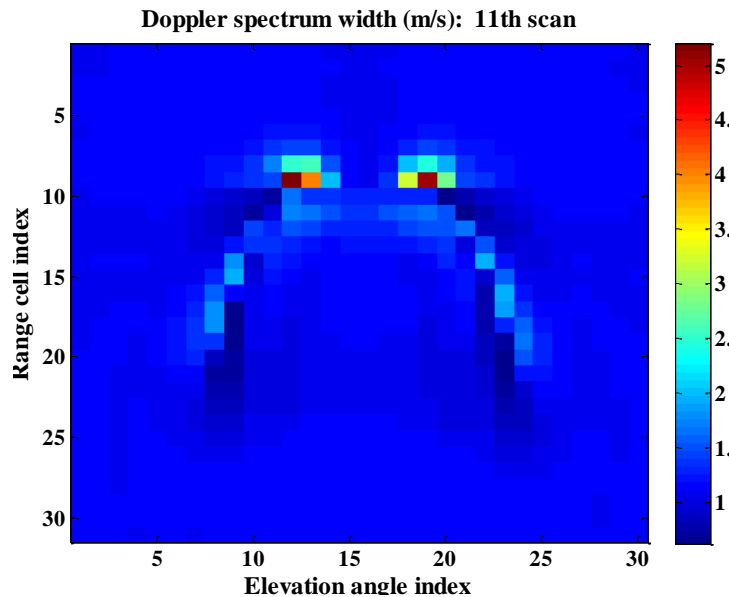




### Wake vortex detection

Given the I & Q radar signal time series from a sequence of radar scans, the procedures for wake vortex detection can be summarized as the following:

- (1) Computation of the Doppler velocity spectrum for raindrops;
- (2) Estimation of the Doppler spectrum width;
- (3) For the Range-Elevation map of Doppler spectrum width of raindrops at each scan, determination of the two radar cells with peak values of Doppler spectrum width by local peak detection algorithms.



### Wake vortex parameter estimation

Wake vortex position

$$\begin{cases} x_1(k) = r_1(k) * \cos(\alpha_1(k)); y_1(k) = r_1(k) * \sin(\alpha_1(k)); \\ x_2(k) = r_2(k) * \cos(\alpha_2(k)); y_2(k) = r_2(k) * \sin(\alpha_2(k)); \end{cases}$$

Vortex separation

$$b_0(k) = \sqrt{r_1(k)^2 + r_2(k)^2 - 2r_1(k)r_2(k)\cos[\alpha_1(k) - \alpha_2(k)]}$$

$$\hat{b}_0 = \frac{1}{N_s} \sum_{k=1}^{N_s} b_0(k)$$

Vortex circulation and descent velocity

$$\Gamma(t) = 2\pi v_d(t) b_0$$

$$v_d(t) = v_{d0} + a_d t$$

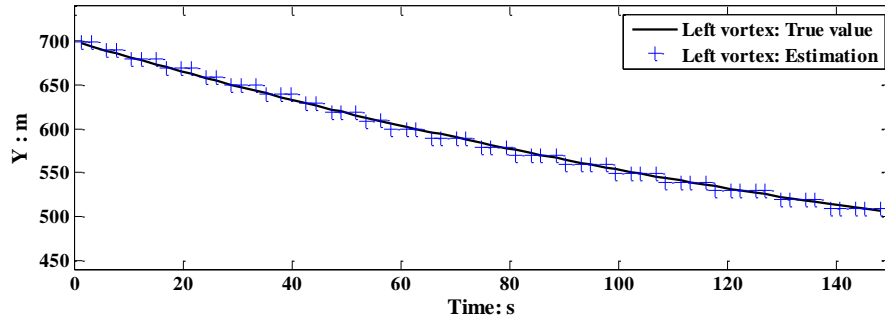
$$y(t) = y_0 + v_{d0} t + \frac{1}{2} a_d t^2$$

$$\begin{cases} \mathbf{y}_1 = [y_1(1), y_1(2) \cdots y_1(N_s)]; & \begin{cases} \mathbf{t}_1 = [t_1(1), t_1(2) \cdots t_1(N_s)]; \\ \mathbf{t}_2 = [t_2(1), t_2(2) \cdots t_2(N_s)]; \end{cases} \\ \mathbf{y}_2 = [y_2(1), y_2(2) \cdots y_2(N_s)]; \end{cases}$$

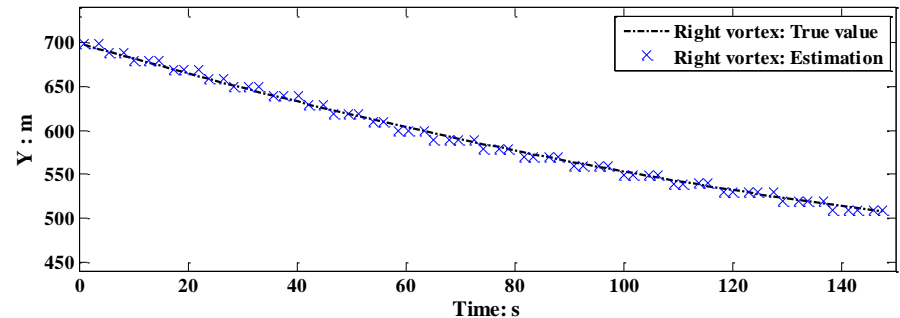
$$\min Q_1(v_{d0}, a_d, y_0) = [y(\mathbf{t}_1) - \mathbf{y}_1]^T [y(\mathbf{t}_1) - \mathbf{y}_1]$$

$$\min Q_2(v_{d0}, a_d, y_0) = [y(\mathbf{t}_2) - \mathbf{y}_2]^T [y(\mathbf{t}_2) - \mathbf{y}_2]$$

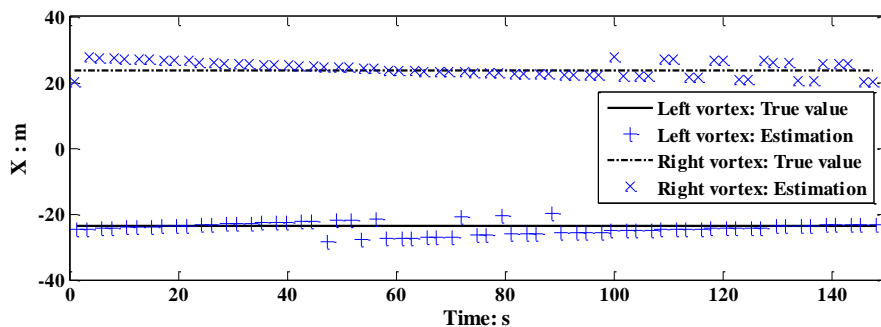
### Estimation of Wake vortex position and vortex separation



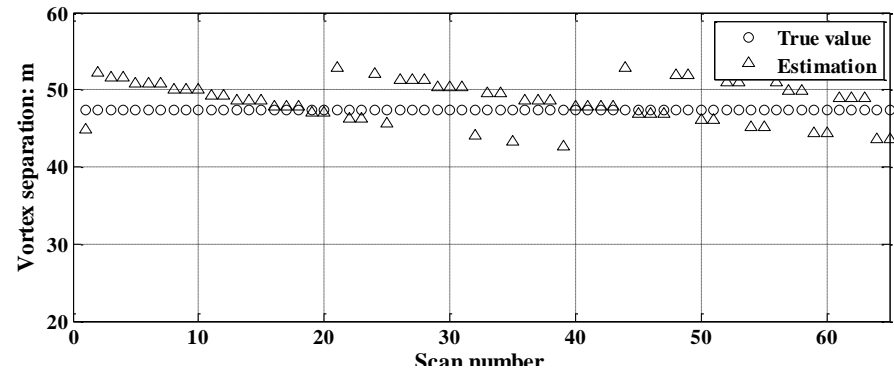
Vertical location of left vortex



Vertical location of right vortex

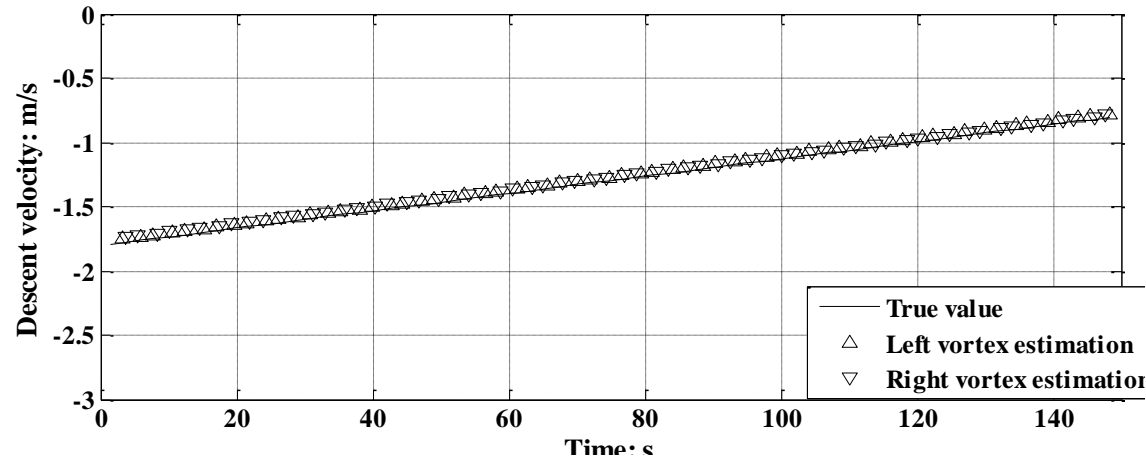


Horizontal location

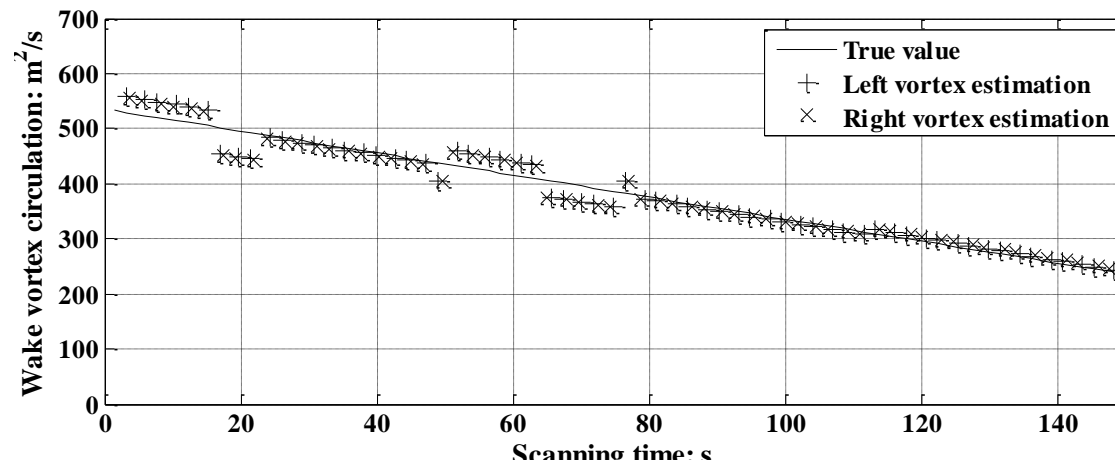


Vortex separation computed from a sequence of scans

### Estimation of descent velocity and vortex circulation



Estimated descent velocity of wake vortex pair (Radar under flight path observation)



Wake vortex circulation estimation



## 5. Conclusions and perspectives

- 5.1 Conclusions
- 5.2 Perspectives

- ❖ The radar signatures of wake vortices in rainy weather have been modeled and analyzed in three successive steps:
  - Computation of the raindrops' motion and distribution
  - Simulation of the radar signatures of raindrops
  - Interpretation of the simulated radar signatures
- ❖ A series of valuable models and methodologies, which can be further exploited for designing new wake vortex radar systems, have been developed, including:
  - A methodology to compute the raindrops' trajectory in wake vortices
  - A methodology to compute the raindrops' distribution in wake vortices
  - A wake vortex radar simulator based on radar signal time series
  - A wake vortex radar simulator based on the raindrops' number concentration and velocity distribution in wake vortices

- A methodology based on the computation of three spectral moments to interpret the radar signatures of raindrops in wake vortices
  - A wake vortex detection method based on the analysis of Doppler spectrum width of raindrops
  - A methodology to estimate the wake vortex characteristics, including the position, vortex separation, descent velocity and vortex circulation
- ❖ The simulation results are consistent with the results of radar trials and the capability of X/W band radar to detect wake vortex in rainy weather have been demonstrated. The raindrops appear to be the “wake vortex tracer”, hence, wake vortex is visible:
- by eyes due to cloud droplets’ motion or contrail
  - by Lidar due to the aerosols’ motion within it
  - by Radar due to the raindrops’ motion within it

- ❖ The analysis of raindrops' motion and distribution can be improved by integrating non-idealized atmospheric characteristics
- ❖ Interaction between raindrops (collision or coalescence) and the effects of raindrops on wake vortex should be further studied
- ❖ The developed radar simulators can be extended to the study of radar signatures of other hydrometeors like fog, cloud or snow
- ❖ Exploitation and upgrade of the radar simulators: optimal radar parameters, on-board detection, polarimetric measurements, GPU parallel computation
- ❖ Wake vortex detection and characterization: detection and false alarm probability, circulation estimation based on the retrieval of wake vortex velocity field from the radar signatures of raindrops in wake vortices



**Thank you for your attention!**